4-28-2023

Understanding Groundwater Flow in a Saturated Buffer Zone (Sbz) Using Numerical Models: Case Study of T 3 Site, Mclean County, Central Illinois

Nnaemeka Henry Nsude
Illinois State University, nnaemeka.nsude@gmail.com

UNDERSTANDING GROUNDWATER FLOW IN A SATURATED BUFFER ZONE (SBZ) USING NUMERICAL MODELS: CASE STUDY OF T3 SITE, MCLEAN COUNTY, CENTRAL ILLINOIS

HENRY N. NSUDE

49 Pages

Loss of nutrients, such as nitrogen and phosphorous, from agricultural lands in the Midwest affects farm productivity and environmental quality. Nutrient runoff from lands discharged into streams degrades the aquatic ecosystem through eutrophication and subsequent hypoxic conditions. The presence of nitrogen also threatens the potability of numerous aquifer bodies globally due to their high solubility in water and through the interaction between surface water and groundwater bodies. To tackle this problem, best management practices such as Saturated Buffer Zone (SBZ) are implemented to reduce nitrogen from nitrate-laden tile water from agricultural lands before being discharged into streams. Groundwater flow and interactions at SBZ are not well understood. To aid the understanding of groundwater flow in the SBZ with the T3 site as a case study, this project aims to understand the interaction between groundwater flow and local tile water flow and the influence of tile water on the groundwater with varying the rate of discharge of tile water. Finite difference groundwater modeling code (MODFLOW) was used to produce a three-dimensional, steady-state groundwater model. After calibration using manual and autocalibration techniques, several scenarios were run with variable tile discharge rates, and the resulting change in groundwater flow direction using particle tracking code - MODPATH was analyzed. The results demonstrated that the influence of groundwater flow on tile flow reduces with a nonlinear (polynomial) trend as tile discharge increases. The field of influence of tile water on local groundwater logarithmically increases as tile discharge increases.

This has a direct implication on the effectiveness of the SBZ in reducing nitrate and hence, their design.

KEYWORDS: MODFLOW, MODPATH, Pilot Point, Saturated Buffer Zone

UNDERSTANDING GROUNDWATER FLOW IN A SATURATED BUFFER ZONE (SBZ) USING NUMERICAL MODELS: CASE STUDY OF T3 SITE, MCLEAN COUNTY, CENTRAL ILLINOIS

HENRY N. NSUDE

A Thesis Submitted in Partial
Fulfillment of the Requirements
for the Degree of

MASTER OF SCIENCE

Department of Geography, Geology, and the Environment

ILLINOIS STATE UNIVERSITY

2023

UNDERSTANDING GROUNDWATER FLOW IN A SATURATED BUFFER ZONE (SBZ) USING NUMERICAL MODELS: CASE STUDY OF T3 SITE, MCLEAN COUNTY, CENTRAL ILLINOIS

HENRY N. NSUDE

COMMITTEE MEMBERS:

Wondy Seyoum, Chair

Eric Peterson

Catherine O'Reilly

ACKNOWLEDGMENTS

My profound gratitude goes to Dr. Wondy Seyoum for serving as my thesis advisor and providing me with a solid foundation and insight throughout the thesis process. You spent countless hours providing me insight into groundwater model building and at the end I can boast of becoming a better hydrogeologist. I would also like to thank Dr. Eric Peterson for serving on my thesis committee and providing a strong background into the physical hydrogeology necessary to ensure a realistic groundwater model. I would also use this opportunity to thank Dr. Catherine O'Reilly for serving on my thesis committee and teaching me how to write and think through the why and how of this thesis. Without you, I probably would not even have finished the program. The three of you have made my sojourn at Illinois State University a fruitful one.

I would also like to thank my friends that made my time at Illinois State University a fruitful one. Particularly appreciation goes to Oghenevwhede Efobo and Okiemute Commander for your insight on map making using ArcMap.

Finally, I would like to thank my family members for always providing support, whether financial or emotional. Appreciation goes to Franklin Nsude and George Nsude for seeing me through my stay in the United States. You made my stay here comfortable in so many ways and for that I am eternally grateful.

H.N.

CONTENTS

	Page
ACKNOWLEDGMENTS	i
CONTENTS	ii
TABLES	iv
FIGURES	v
CHAPTER I: INTRODUCTION	1
1. Questions and Hypothesis	7
CHAPTER II: STUDY SITE	9
CHAPTER III: METHODS	13
3.1 Conceptual Model	13
3.2 Numerical Model Design	15
3.3 Model Calibration and Uncertainty Quantification	17
3.4 Scenarios	21
CHAPTER IV: RESULTS	23
4.1 Calibration	23
4.2 Model Uncertainty Quantification (Parameter Randomization)	26
4.3 Scenario Analysis	27
CHAPTER V: DISCUSSION	34
5.1 Calibration	34
5.2 Scenarios	34
5.3 Limitations	36
CHAPTER VI: CONCLUSIONS	38
REFERENCES	40

APPENDIX 49

TABLES

Table		Page
1.	Data used for study	13
2.	Parameters used for calibration	20
3.	Parameters used for stochastic randomization	21
4.	Post calibration parameters and values	26

FIGURES

Figure	Page
1. The Terrestrial Nitrogen Cycle	3
2. Location of study site, observation wells 2, 4, 6, 8, 10 and 12 have nested wells A-D in order of decreasing depth	10
3. Site soil stratigraphy (Miller et al., 2018)	11
4. Water Table Elevation at T3 site	12
5. 2D sketch of conceptual model	15
6. Conceptual model showing boundary conditions, grid design and location of diversion Tiles	17
7. Figure showing location of pilot points	19
8. Flowchart describing groundwater modeling process	22
9. Figure showing model with calibrated hydraulic heads	24
10. Plot showing observed versus computed hydraulic heads	24
11. Plot showing residual versus observed hydraulic heads	25
12. Relative sensitivity plot	25
13 (a). Mean head for sand/gravel unit	27
(b). Mean hydraulic conductivity for sand/gravel unit	27
14. Picture showing defined contributing particle width	28

15. Picture showing backward particle flow path lines for 40 m^3/day, 48 m^3/day, 100 m^3/day and 200 m^3/day tile discharge, respectively 29

16. Plot showing groundwater contributing area per width versus tile discharge 30

17. Picture showing defined near and far field influence 31

18. Figure showing near and far field particle path lines for 40 m^3/day, 48 m^3/day, 100 m^3/day, and 200 m^3/day tile discharges, respectively 32

19. Plot showing the field of influence versus tile discharge 33

20. Cross-sectional view of groundwater model with tile discharge at 200 m^3/day (Exaggeration: X10) 36

CHAPTER I: INTRODUCTION

The concentration of nitrate is naturally very low in water bodies, but today it is the most common source of nonpoint source of pollution to surface water bodies in the United States (Carpenter et al., 1998). This is due to various human activities, particularly the extensive use of fertilizers for crop production that has led to an increase in nitrate concentrations in water bodies. The extensive use of fertilizers to sustain good yield in agriculture has contributed to significant load of nitrogen entry into water bodies. The use of nitrogen fertilizers for crop farming has led to high nitrate content in water discharged to streams, which degrade aquatic ecosystems through process of eutrophication and subsequent hypoxic conditions (Galloway et al., 2008, Rosenstock et al., 2014).

Agricultural activities, specifically the planting of corn, soybeans, and wheat, are extensive and a huge contributor to the economy of Illinois, contributing $17 billion to state economy (source: https://cropinsuranceinamerica.org/illinois/). In McLean County where the city of Bloomington is located, agricultural activities represent 3% of state agriculture sales at $457.06 million (USDA-NASS: Census of Agriculture, 2017). However, the farm fields in central Illinois can become waterlogged because of the soils' high-water retention capacity. This is because the soils in the central Illinois area are composed of organic-rich clay loams, which are known to have very good water-withholding capacity (Collman, 2004). As a result, tile drainage is used to channel the water into nearby streams to improve crop yield & accessibility of fields (Miller et al., 2018). The tile-drained water contains high concentration of nutrients from agricultural lands in the area, which ends up in streams locally, and drains into the Mississippi River watershed. David and Gentry (2000) estimated that between 15 and 20% of the total nitrogen in the Gulf of Mexico from the Mississippi River watershed comes from Illinois.

The focus of this study is the T3 site, which is a saturated buffer zone (SBZ) created by diverting tile water draining agricultural land. A diversion system was created in a restored prairie in central Illinois to channel the water into a riparian buffer zone and hopefully, have the nitrate significantly reduced before it gets into the nearby stream. The riparian zone refers to the land adjacent to streams, rivers, or other surface water bodies where vegetation is highly influenced by the presence of water (Lasagna et al., 2016). They are a type of edge-of-field nitrate reduction practice. They aid in filtering waste (nutrients and pesticides) produced from agricultural activities and are recommended as best management practice (BMP) by the US Environmental Protection Agency (EPA) for nutrient load reduction prior to water entry into streams (Mayer et al, 2006). Some of the nutrient load reduction processes for nitrate include denitrification, dilution, plant uptake etc. As such, there is a need to better understand the SBZ with respect to the interaction between groundwater flow and local tile water flow. This information will be useful to farmers, land managers, and government agencies to design better tools/methods for land use/water management.

To understand nitrogen transport in water, it is important to refer to the nitrogen cycle. The nitrogen cycle describes how nitrogen is transformed into different chemical forms as it circulates between the atmosphere and the terrestrial environment (Figure 1). It consists of 5 processes: fixation/volatilization, mineralization, nitrification, immobilization, and denitrification. Fixation describes the process whereby nitrogen gas is converted to nitrite and nitrates. This occurs naturally when lightning provides the energy needed for oxygen to react with nitrogen to produce nitrogen oxide and nitrogen dioxide or artificially through fertilizer manufacturing process where atmospheric nitrogen is combined with hydrogen to produce ammonia and subsequently ammonium nitrate (Peoples et al., 1995). These forms of nitrogen are then fixed to soils by nitrogen

fixing bacteria that may have a symbiotic relationship with the plants or may be free living. During the second phase (mineralization), organic nitrogen from decomposing plants and animals are transformed by microbes to ammonia which is converted to ammonium when it reacts with water. Ammonium is held by soils and used by plants that cannot get their nitrogen from the nitrogen fixation process. In the third step (nitrification), ammonium ions are converted to nitrites by aerobic nitrifying bacteria, *Nitrosomonas* and the nitrites are subsequently converted to nitrates by aerobic nitrifying bacteria, *Nitrobacter* (Manahan, 2010). Immobilization describes the process where microbes take in ammonia and ammonium, thus removing the nitrogen from the soil and in some cases leading to nitrogen deficiency. Immobilization and mineralization run counter to each other, and they control the net amount of nitrogen in soils. The last stage, denitrification, describes the biochemical process where nitrate is converted to nitrogen or nitrous oxide and is returned to the atmosphere where the cycle was initiated.

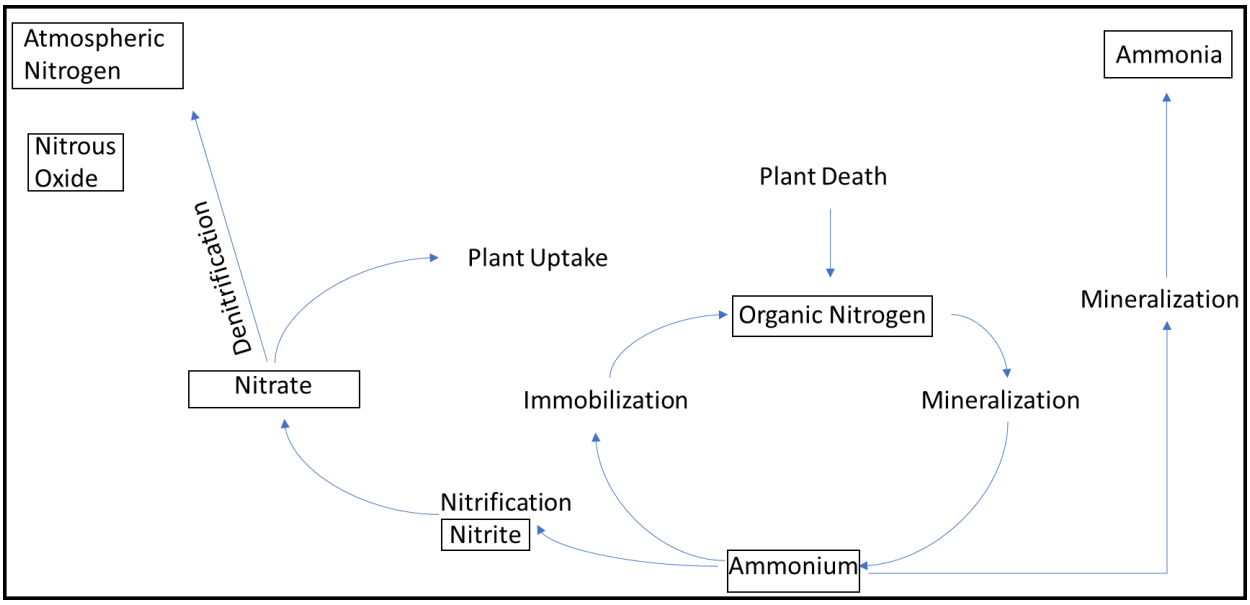

Figure 1: The Terrestrial Nitrogen Cycle

Denitrification represents the process by which the nitrate is converted into nitrogen gas (Groh et al., 2019). Here, the nitrate is completely removed from the soil-water system. As a result of spatiotemporal heterogeneities in distribution of oxygen, carbon sources, and NO_3^- in the riparian zone, denitrification is not uniform but rather there exists hot spots in riparian areas where denitrification most takes place (McPhillips et al, 2015). The nitrate reduction reaction can be expressed as a half-equation:

$$2NO_3^- + 12H^+ + 10e^- \rightarrow N_2 + 6H_2O$$ (Tesoriero et al., 2000)

Two main factors have been shown to favor the rate of denitrification (Rivett et al., 2008, Anderson et al., 2014). These include: (1) the occurrence of nitrate, denitrifying bacteria, and electron donor (organic carbon, reduced iron, or reduced Sulphur) and (2) Anaerobic environment (dissolved oxygen concentrations < 1-2 mg/l). Other conditions that play a secondary role in the rate of denitrification include:

- Optimum temperature conditions (between 25-35 ^{0}C): it has been shown that a 5 ^{0}C increase in temperature leads to 10 times increase in denitrification rate (Rivett et al., 2008),
- Low redox values, between 200-300 mV that implies anaerobic conditions (Vidon and Hill, 2005) and pH values between 5.5 to 8.0 (Rivett et al., 2008),
- Large pore size (at least >1 μm) for microbial population to grow (Rivett et al., 2008),
- Low salinity, ideally < 4 g/l chloride to enable microbial activity (Ucisik and Henze, 2004),
- Absence of inhibitory substances, i.e., heavy metals & pesticides (Rivett et al., 2008), and
- Optimal width of buffer zone between 11-15 m to supply more areas where groundwater conditions will favor denitrification (Lyu et al., 2021)

Residence time is a key metric for understanding the role denitrification plays in groundwater systems (McPhillips et al., 2015). Residence time quantifies the amount of time water has stayed in each portion of the hydrologic cycle (Eby, 2004). Long residence time allows enough time for microbial and biochemical processes needed to convert nitrate to nitrogen gas and hence, to eliminate them from the water system. Using computations of groundwater velocity, Streeter and Schilling (2021) demonstrated that denitrification could potentially remove tile nitrate input in less than a day. Sahad (2022) used tracer test to establish the average residence time in the SBZ at T3 site to be 27 days. The rate of denitrification follows a seasonal pattern increasing in spring and winter and reducing in fall and summer due to reducing water table, which leads to less contact between nitrate laden water and organic rich topsoil (Hill, 1996). The reduction in water table during fall and summer is because of increase in evapotranspiration.

In dilution, the nitrate concentration is reduced through the process of tile water mixing with groundwater of different solute concentration, although it does not eliminate the nitrate. As a result, the overall mass of nitrate is masked (Lasagna et al., 2013). A key metric for understanding the role of dilution is through estimation of the volumetric flow rate per unit width perpendicular to flow direction (q_u), which is a function of the product of hydraulic conductivity (K), hydraulic gradient (i), and aquifer thickness (b). Studies have shown that the higher the q_u the lower the output contaminant concentration (Lasagna et al., 2013; Lasagna et al., 2016).

Previous study by Brooks & Jaynes (2017) illustrated how saturated buffers in the Midwest (Iowa, Illinois, and Minnesota) were effective in reducing nitrate load by 61% on average and are cost-effective (average: $2.44 per lb.-Nitrogen) compared to other field edge practices for nitrate reduction. Jaynes and Isenhart (2014) suggested that riparian buffers remove nitrate by plant uptake, denitrification, and microbial immobilization. They also confirmed SBZs are cost-

effective alternative ($2.17 per kg-N) compared to wetlands ($3.26 per kg-N). Jaynes and Isenhart (2019a) described how saturated riparian buffers removed about 73 kg Nitrogen/year from tile which amounts to 8-84% of nitrate delivered from tile water. McEachran et al (2020) showed that the effectiveness of the saturated riparian buffers is dependent on designing an optimal buffer width to maximize flow of tile water while maintaining sufficient residence time. However, uncertainty exists as to the relationship between the known nitrate reduction mechanisms and groundwater flow (Chen and MacQuarrie, 2004). Groh et al (2019) estimated the saturated riparian buffer to reduce nitrate load by 27-96%, with denitrification responsible for 3.7-77.3% of nitrate load reduction, and vegetation uptake suggested as a possible mechanism for the remaining percent decrease in nitrate. They also showed how an increase in water table led to an increase in nitrate reduction through denitrification. Some authors have shown that in shallow aquifers, dilution plays a dominant role in NO_3^- reduction by masking the overall concentration of the nitrate (Molénat and Gascuel-Odoux 2002, DeLuca and Lasagna, 2005).

Previous work on the T3 site has shown plant uptake playing a role in nitrate reduction in the SBZ, with nitrate concentration reducing in the spring and summer periods and increasing during the fall and winter periods (Miller et al., 2018). Bosompemaa et al (2021) examined the role of plant uptake within the vadose zone of a saturated buffer in nitrate reduction. They showed that plants act as a temporary sink in which nitrogen is continually recycled. Work done by Sahad, 2022, using end member mixing model also demonstrated evidence of nitrate loss at the T3 site. However, his study showed the possibility of upwelling as seen from wells close to the stream that cannot be explained by the end member mixing model. The end member mixing model has not provided the pathway of tracer movement especially in relation to groundwater flow. It tells us the start and end point of tracer but gives no indication as to its pathway. Also, by its nature, it ignores

some important contaminant transport processes, particularly dispersion. Hence, there is a need for further investigation of the subsurface flow using a groundwater model that captures the influence of groundwater flow on local tile water flow and vice versa.

This study focuses on how numerical modeling can be a useful tool in providing insight into groundwater flow in the SBZ. Most groundwater flow models for SBZ are typically one or two-dimensional. Advice on the design of SBZ by the US Department of Agriculture Natural Resource Conservation Service is based on a one-dimensional form of Darcy's Law (McEachran, 2020). McEachran et al, 2020 assumed a one-dimensional form of Darcy's Law in the design of the optimal width of buffer zones for six sites in Iowa. Jaynes and Isenhart (2019b) used a two-dimensional model to investigate the effect of adding an additional distribution pipe on infiltration rate and residence time. This assumption is not always valid because groundwater flow around the stream and around the pipe is three dimensional and thus not captured by these models. Thus, there is a need for a three-dimensional model that describes fluid flow in the SBZ. Uncertainty in groundwater flow has implications for the design of SBZ and correspondingly its ability to effectively remove nitrate and improve surface water quality. This is because it produces an error in the estimate of travel time, which is crucial in understanding the quantity of nitrate that can be removed in the SBZ. McEachran (2020) computed an error of 11.6% in the estimate of travel time associated with a one-dimensional approximation of Darcy's law. The author also developed a three-dimensional homogeneous anisotropic steady-state model for a SBZ in Iowa. However, the model does not capture the heterogeneity typically inherent in the subsurface.

1. *Questions and Hypothesis*

The overall goal of this study is to understand the interaction between groundwater flow and tile water. The specific research questions this study attempts to address are:

1) How does groundwater flow pattern influence the tile water?
2) What is the field of influence of groundwater?

We hypothesized that the influence of tile water on the local groundwater is significant, and the influence increases as the rate of discharge of tile water increases.

CHAPTER II: STUDY SITE

The study site (also known as the T3 site) is a grassy riparian buffer area located in McLean County, central Illinois (Figure 2). It collects tile flow from agricultural land located to the east of the site. The T3 site is equipped with an agricultural runoff treatment system that diverts the tile flow into the subsurface of the riparian buffer. A rerouting system was found 1m below ground with three perforated pipe channels that direct the tile drained water into the subsurface of the SBZ, while the remaining volume is discharged directly into the stream. The perforated rerouted pipes channel flow into the saturated buffer zone 20–35 m upgradient from the stream. This buffer zone allows tile discharge to infiltrate into the soil.

The diversion box is composed of three chambers separated by a set of stoplogs. The stoplogs are used to control the elevation of the water flowing from the upstream chamber to the middle chamber and from the middle chamber to the downstream chamber and subsequently to the stream. In the study site, there are thirty-five observation wells with a 0.75 m screen installed in each. One set, which is parallel to the groundwater flow, consists of 6 sets of nested wells, namely Well 2,4,6,8,10 and 12 with four wells (A-D) at each nested station. The C and D have depths of 2.3 and 1.5 m, respectively, and are for monitoring shallow (from 0-2 m depth) groundwater. The A and B wells are installed to a depth of 3.8 m and 3.0 m, respectively, and are for monitoring deep (depth below 2 m) groundwater. The other sets of wells are composed of eleven individual wells screened at 2.3 m.

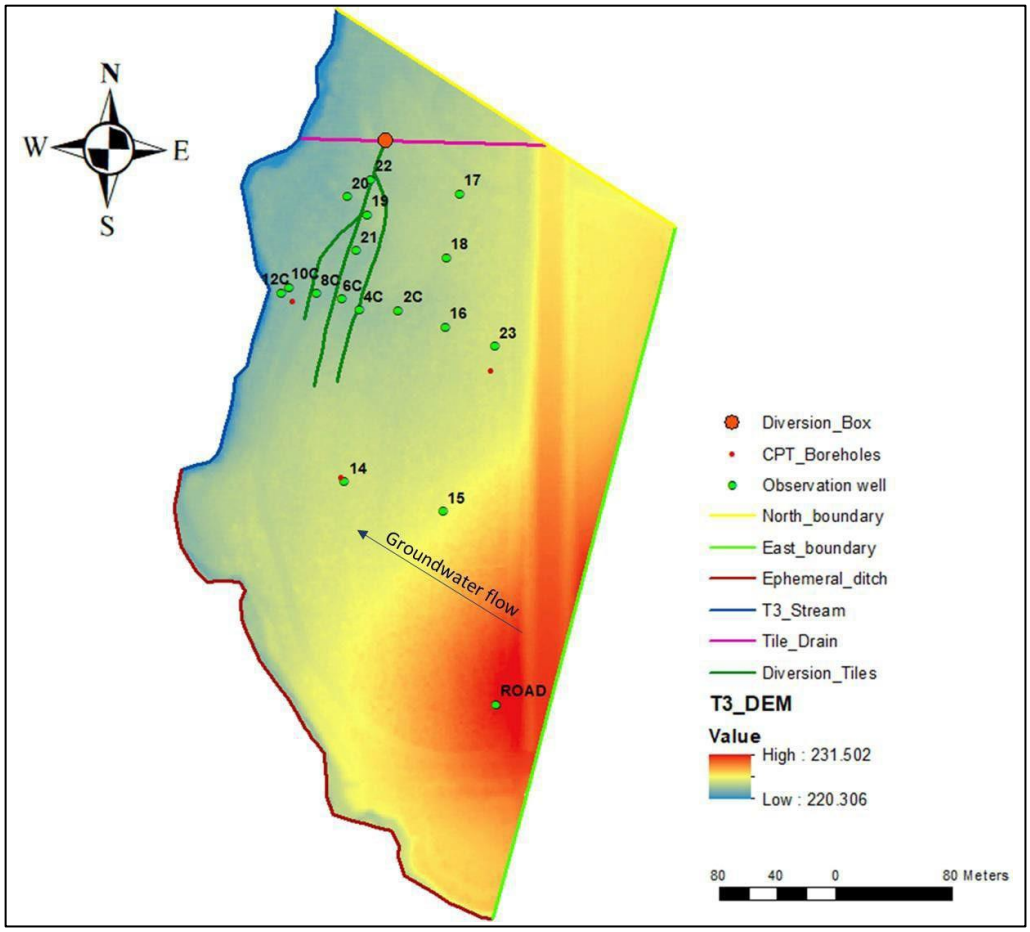

Figure 2: Location of study site, observation wells 2, 4, 6, 8, 10 and 12 have nested wells A-D in order of decreasing depth.

The SBZ is sub divided into 3 lithological layers (Figure 3). At the bottom (below 2m) is a 30-45 m thick blue-grey mud matrix diamicton that is thought to form part of the Wedron Formation, which terminates at the Silurian bedrock (Bosompemaa et al, 2021; Miller et al, 2018). This interval is overlain by a gravely coarse sandy silt (1.5-2 m depth) with spatially varying thickness. This is also the interval where groundwater flow is predominant. Above this interval lies a clay unit (0.66-1.5 m depth) consisting of clay, silty clay, and sandy clay. The clay exhibits increasing sand and gravel gradation with depth (Miller et al, 2018). The clay unit is overlain by a dark rich organic topsoil (0-0.63 m). For this study, we are interested up till the bottom of the

gravely silt with sand unit, as the diamicton does not contribute to flow. This lower boundary will be determined from analysis of cone penetrometry and hydraulic profile data acquired from Illinois State Geological Survey (ISGS). Preliminary analysis of this data puts the no flow boundary in the z-direction at approximately 5 m from surface (Appendix 1).

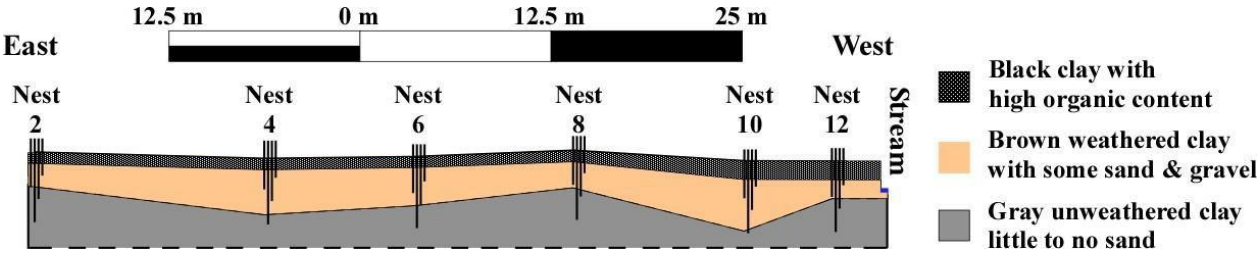

Figure 3: Site soil stratigraphy (Miller et al., 2018)

In general, the topography of the riparian zone gently slopes from east to the W–NW away from the agricultural area towards the stream; groundwater flows in the W–NW direction toward the stream, as displayed in Figure 4. The tiles usually have flows from late winter (March) to late spring (end of May to early June) and in fall. Sustained flow in the tiles corresponds to the period when there is enough recharge and enough contribution of tile flow from agricultural land due to precipitation. The average hydraulic conductivity (K) of the materials obtained from the tracer test ranges from 1.15×10^{-4} m/s to 3.29×10^{-3} m/s (Sahad, 2022), while hydraulic conductivity of the diamicton is estimated at 10^{-9} m/s. With respect to climate, the study site is in a temperate region. The 60-year average annual air temperature is 11.2 °C with a monthly average variance of 30 °C influenced by season (Changnon et al., 2004). The average precipitation (yearly) is 950 mm ± 100 mm, with 40-year monthly average showing the greatest precipitation occurs in the spring, and the lowest precipitation occurs in winter (Changnon et al., 2004).

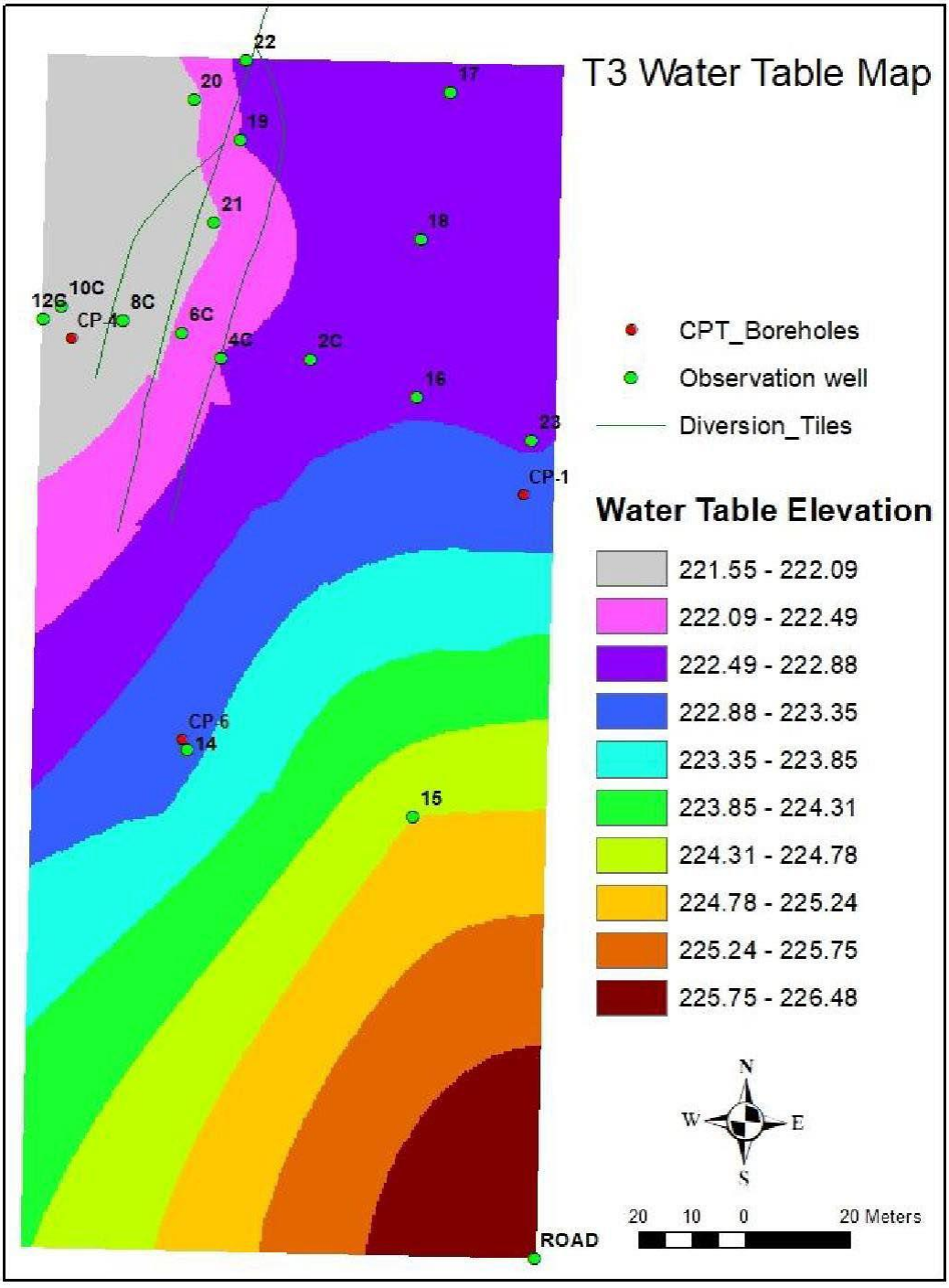

Figure 4: Water Table Elevation at T3 site

CHAPTER III: METHODS

3.1 Conceptual Model

A 3-dimensional model representing flow in the SBZ was developed using MODFLOW 2000 code using GMS as a graphical user interface. First, a stratigraphic model of the SBZ was built, combining all field data from the project area, i.e., a 1-meter LiDAR Digital Elevation Model (DEM), borehole logs from cone penetrometry test, slug test data, drilling well log data, surface water elevations, etc. into a hydrogeologic conceptual model of the SBZ (Table 1). The slug test provides data that is used to derive hydraulic conductivity within the vicinity of the piezometers.

Table 1: Data used for study.

Data Collected	Date Collected
Cone Penetrometry and Hydraulic Profile (CP-1, CP-4 AND CP-6): Illinois State Geological Survey	April 2022
Slug Test (Wells 2C, 2D, 4C, 4D, 4C, 6C, 6D, 8C, 8D, 10C, 10D, 12C, 12D, 13, 14, 19, 22, 23 ROAD)	2015 – 2021
Depth to Water Measurements (Wells 12C, 10C, 8C, 6C, 4C, 2C, 14, 16, 17, 18, 19, 20, 21, 23)	February 4, 2023
Topographic Map (DEM – LiDAR): Illinois GIS Clearinghouse	2011

The main idea is to be able to generate a model that describes the distribution of hydraulic head and groundwater flow rates in the SBZ. The model consists of 4 boundaries, where the stream considered as the specified head boundary to the west and the outer edges of the farm fields as the boundaries to the east, which was also assigned a constant head boundary. The boundary values for the stream were determined from the digital elevation model (DEM), while the boundary at the east was determined from the groundwater level contour map using in situ observation data (Figure 4). The discharge box (adjusted by a few meters to account for boundary effect) acted as a no flow boundary in the north region, while an ephemeral ditch was used as a no flow boundary in the south region. With depth (at the z-direction), a no flow boundary was assumed at the interface between the sand/gravel unit and the diamicton. This lower boundary was determined from analysis of cone penetrometry and hydraulic profile data acquired from Illinois State Geological Survey at 220 m below mean sea level (Figure 5).

Recharge and water input from the diversion tile constitutes the source in the 3D model while discharge to the stream constitutes the sink for the study area. The diversion tile was represented as a polygon depicting the shape of tiles and injection wells placed in the cells

corresponding to the polygon representing the diversion tiles. Tracer test results indicated that there is no evidence of flow at the eastern segment of the tile drain (Sahad, 2022). As such, the injection wells were placed only on the middle and western segments of the diversion tiles (Figure 6).

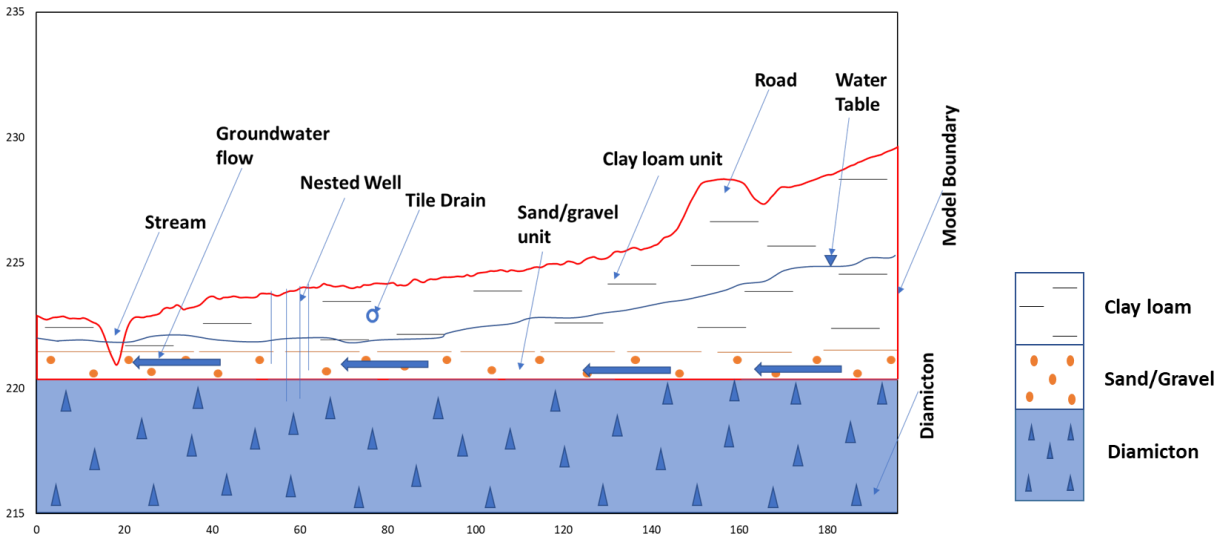

Figure 5: 2D sketch of conceptual model.

3.2 Numerical Model Design

Next, the hydrogeologic conceptual model was transformed into a numerical model using the finite difference flow Model, MODFLOW, with appropriate numerical properties, boundaries, and observations. The numerical model captured the 2 layers depicting the intervals of interest. A digitized map of the T3 site was superimposed on the model as the top of the model. Due to paucity of borehole data, the bottom of the clay loam unit was estimated uniformly at 221.5 m below mean sea level, while the bottom of the sand/gravel unit was estimated uniformly at 220.0 m below mean sea level. Steady-state flow condition was simulated representing the condition on the 4th of

February 2023, where there was no tile flow. The system is assumed to be heterogeneous and anisotropic since deposits at the T3 site were formed from glacial retreat process (Weedman et al., 2014). These deposits are usually associated with significant heterogeneity. A constant head boundary condition of 0.72 m (Head-Stage from 221.12 to 220.4 m) was used to model water level at the stream (western zone), while a constant head boundary condition of 3.8 m (Head Stage from 226.6 to 222.8 m) was applied at the eastern zone to simulate incoming groundwater flow. Recharge, which crossed the top boundary at a constant rate, was initially set at 0.000261 m/day, which is approximately 10% of average annual precipitation. The 10% of average annual precipitation was used in groundwater flow models of areas with similar geology by Van der Hoven et al (2008) and Ludwikowski and Peterson (2018). Using local grid refinement, grid spacing is 0.2 meter in both x and y directions around the diversion tile up to 2m throughout rest of model. Porosity was assumed as 30% for all lithologies. The governing equation for steady-state heterogeneous anisotropic groundwater flow equation condition is:

$$\frac{\partial}{\partial KK}(KKKK.\frac{\partial h}{\partial KK}) + \frac{\partial}{\partial KK}(KKKK.\frac{\partial h}{\partial KK}) + \frac{\partial}{\partial KK}(KKKK.\frac{\partial h}{\partial KK}) + WW = 0 \quad \ldots\ldots\ldots\ldots\ldots\ldots\ldots\ldots (1)$$

Where K is the hydraulic conductivity, x,y,z represents orthogonal coordinate directions while W represents source/sink .

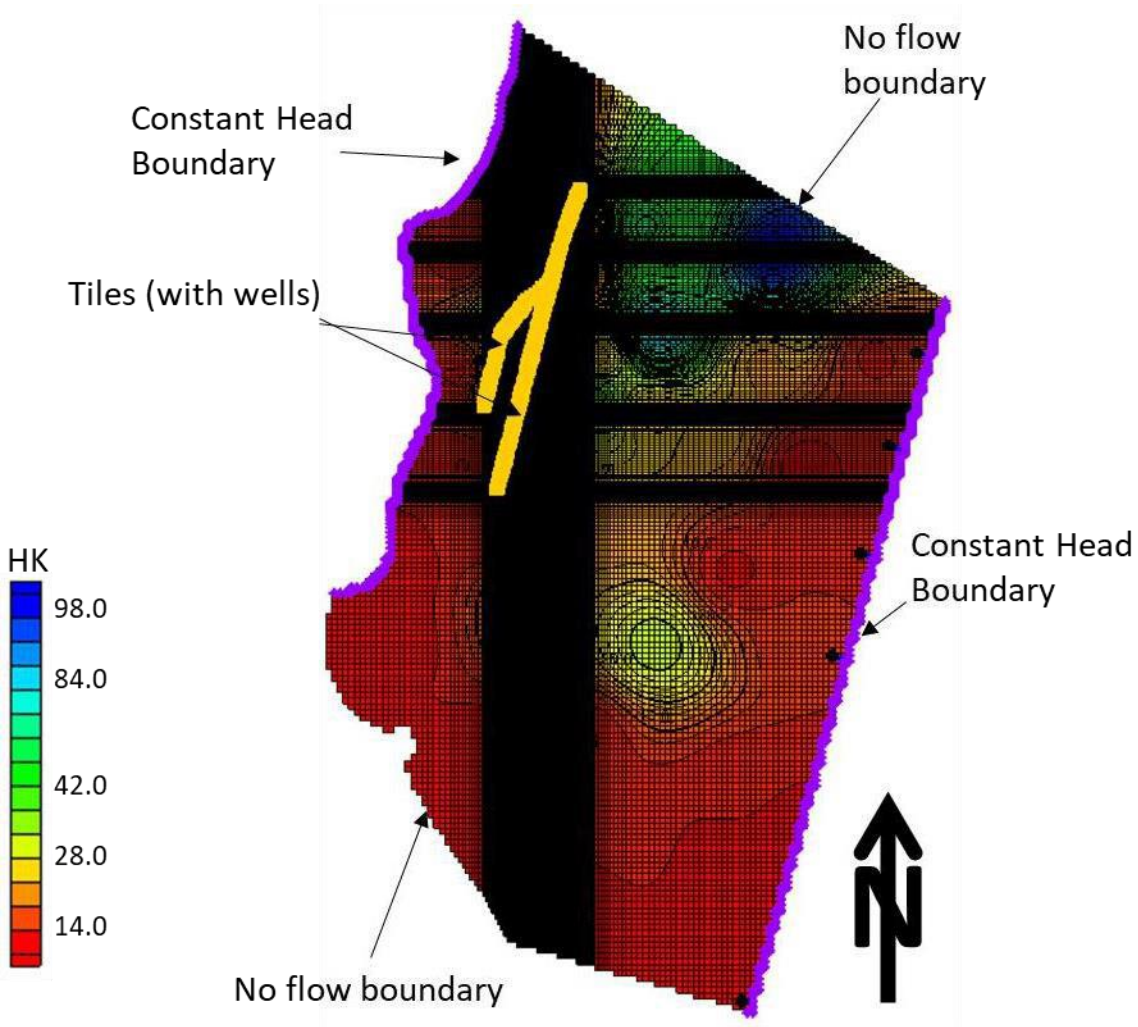

Figure 6: Conceptual model showing boundary conditions, grid design and location of diversion tiles; HK – horizontal hydraulic conductivity (m/day).

3.3 Model Calibration and Uncertainty Quantification

The numerical model was run to simulate hydraulic heads and model output (hydraulic head) was calibrated to field observations using head data from 14 observation wells. Model calibration involved adjusting recharge, hydraulic conductivity, and vertical anisotropy parameters to reduce errors between simulated and observed heads. First, calibration was done manually (using the trial-and-error approach). Subsequently, an automated calibration using PEST was

conducted. Calibration of hydraulic conductivity for the clay loam unit, recharge and vertical anisotropies of the clay loam unit and the sand/gravel unit was done using the zonal approach.

To capture heterogeneity in the sand/gravel unit, hydraulic conductivity in this aquifer was calibrated using the pilot point method (Figure 7). The pilot point method is an inverse modeling technique that uses a 2D scatter point set to iteratively estimate parameters (e.g., recharge or hydraulic conductivity) in the pilot points within a defined domain. Once the objective function has been minimized at the calibration targets (e.g., observation heads), spatial interpolation to all active cells within the domain is performed using inverse distance weighted or kriging technique. Pilot points aid in capturing heterogeneity in groundwater systems without the challenge of numerical instability in fields with limited observation data (Doherty and Hunt, 2010). For this study, 46 pilot points were liberally placed within the sand/gravel interval with increased spatial density in areas with a high concentration of observation wells (Figure 7). The parameter estimation software suite (PEST) by Doherty 2020a, 2020b was used in the estimation of appropriate values for the pilot points.

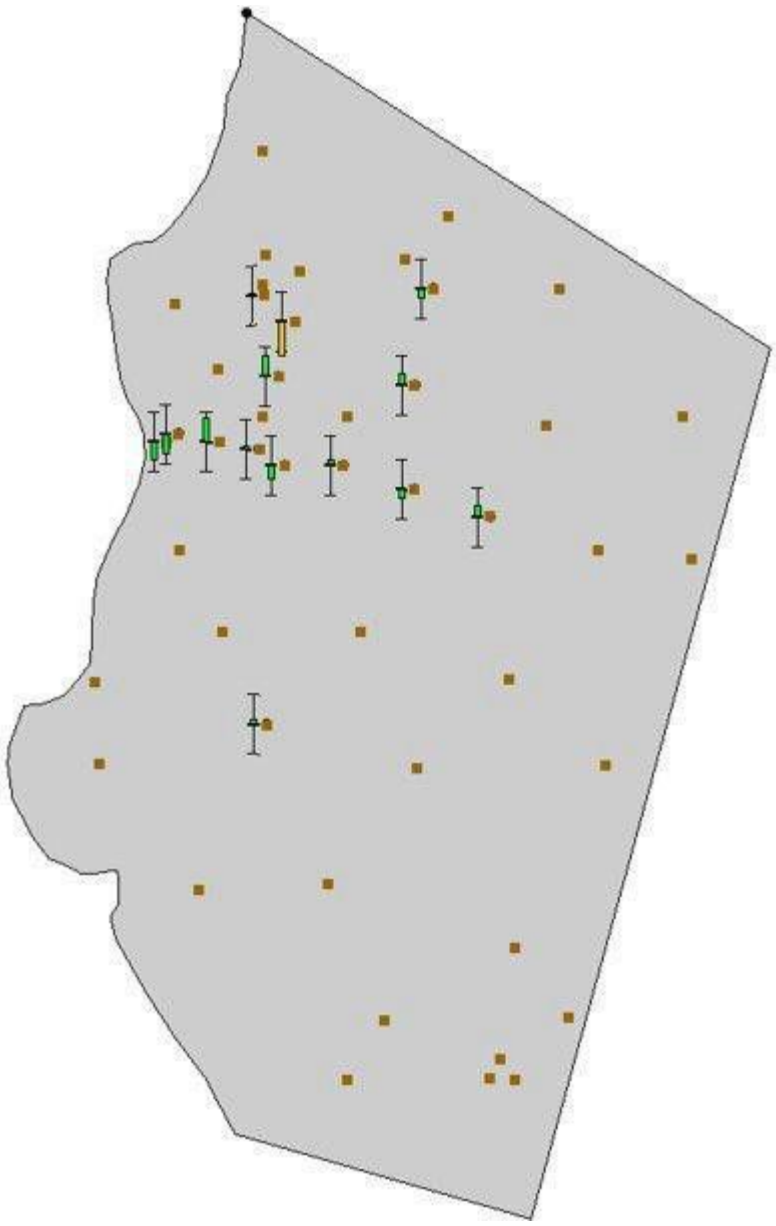

Figure 7: Figure showing location of pilot points.

The pilot points were used in conjunction with regularization (Tikhonov regularization with single value decomposition), thereby allowing for the use of parameters that greatly exceed the number of observations and ensuring numerical stability of model (Doherty, 2003). The liberal use of pilot points exceeding observation points also reduces the impact of pilot point placement and interpolation technique on the accuracy of the calibration process (Doherty, 2003 and Hunt et

al., 2007). Inverse distance weighted technique was used to interpolate to all active cells within the sand/gravel domain. This interpolation technique assumes that the interpolating surface would be influenced more by nearby points as compared to points farther away. The parameter values initially used for the calibrated model are listed in Table 2. The model was calibrated up to 95% confidence interval and observed head interval of 0.2 m.

Table 2: Parameters used for calibration.

Parameter	**Value**	**Minimum**	**Maximum**
Horizontal hydraulic conductivity – clay loam (m/day)	0.3	0.01	1
Horizontal hydraulic conductivity – sand/gravel (m/day)	35	0.1	100
Recharge (m/day)	0.000261	0.00001	0.001
Vertical Anisotropy – clay loam	10	1	100
Vertical Anisotropy – sand/gravel	10	1	100

Table 3: Parameters used for stochastic randomization.

Parameter	**Mean Value**	**Minimum**	**Maximum**	**Standard Deviation**	**Distribution**
Hydraulic conductivity – clay loam (m/day)	0.182	0.01	1	0.5	Normal
Hydraulic conductivity – sand/gravel (m/day)	Pilot Point	0.1	100	20	Normal
Recharge (m/day)	0.000693	0.00001	0.001	0.8	Normal
Vertical Anisotropy – clay loam	2.64	1	100	20	Normal
Vertical Anisotropy – sand/gravel	52.202	1	100	20	Normal

3.4 Scenarios

Using the calibrated model, 10 scenarios were run to quantify the influence of tile flow on local groundwater flow and to understand how groundwater flow patterns influence the local groundwater flow and tile water. Each scenario representing tile discharge at specific volume per day (0.063 m^3/day, 10 m^3/day, 20 m^3/day,30 m^3/day,40 m^3/day, 48 m^3/day, 50 m^3/day, 100 m^3/day, 200 m^3/day and 500 m^3/day) into the SBZ was represented as specified flow. In each scenario, 1 particle was placed at each injection well representing the diversion tile and a backward run was

performed to understand the effect of groundwater flow on local groundwater flow and tile flow. To quantify the influence of tile flow on local groundwater flow, 1233 particles were placed near diversion tiles in an orientation approximately perpendicular to the tiles and parallel to the no flow boundaries and a forward run performed.

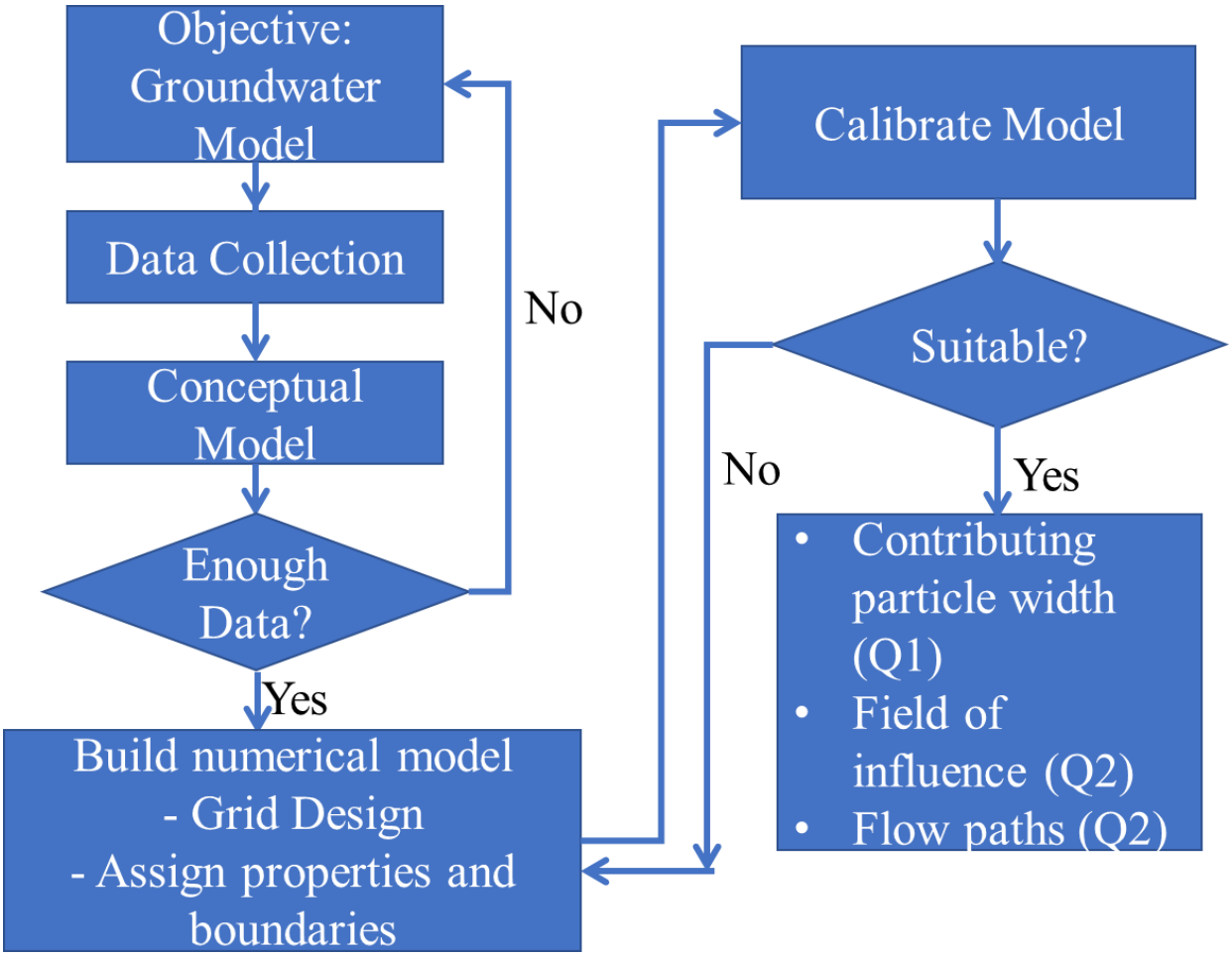

Figure 8: Flowchart describing groundwater modeling process.

CHAPTER IV: RESULTS

4.1 Calibration

In general, the model reproduces the observed hydraulic heads except for well 19, with a residual head of about 0.22 m (Figure 8). The mean error (ME), mean absolute error (MAE), and root mean square error (RMSE) heads are 0.01 m, 0.09 m, and 0.11 m, respectively. A plot of computed versus observed head shows a high degree of correlation with $R^2 = 0.95$ (Figure 9), while a plot of residual versus observed head yields a low degree of correlation of 0.002 (Figure 10). Statistically, RMSE of 0, R^2 of 1 and random distribution of residuals ($r = 0$) would represent a perfect match between computed and observed values. Random distribution of residuals also depicts absence of bias in groundwater model (Reilly and Harbaugh, 2004). Relative sensitivity analysis shows that hydraulic conductivity of the sand/gravel unit as the most sensitive parameter followed by the recharge, while vertical anisotropies of the clay and sand/gravel unit are the least sensitive parameters (Figure 11). Sensitivity describes the model response to varying input parameters (such as recharge or hydraulic conductivity) on target variable (hydraulic head) while relative sensitivity quantifies the percentage of impact of a parameter in relation to other parameters. Post calibration values for hydraulic conductivity, recharge and vertical anisotropies are displayed in Table 3.

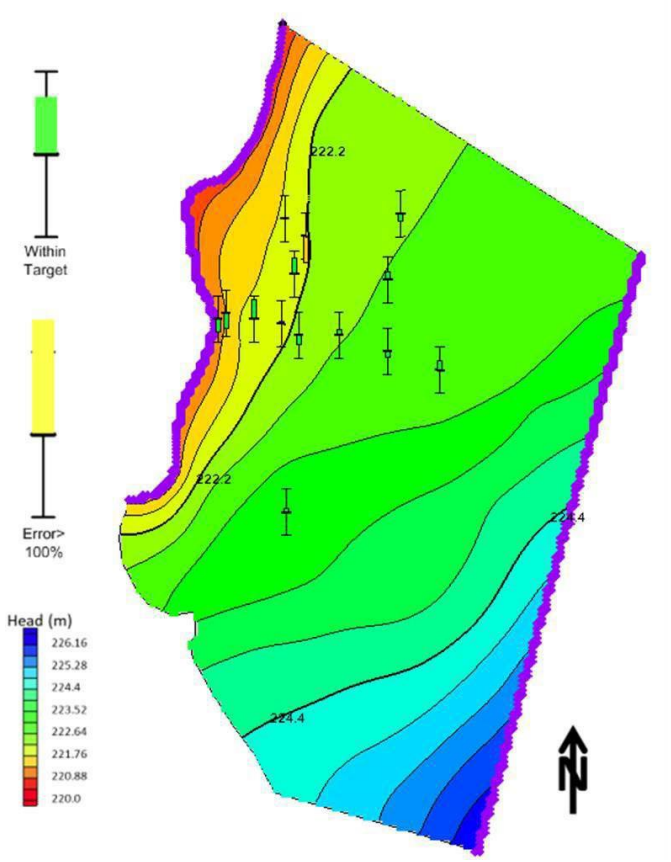

Figure 9: Figure showing model with calibrated hydraulic heads.

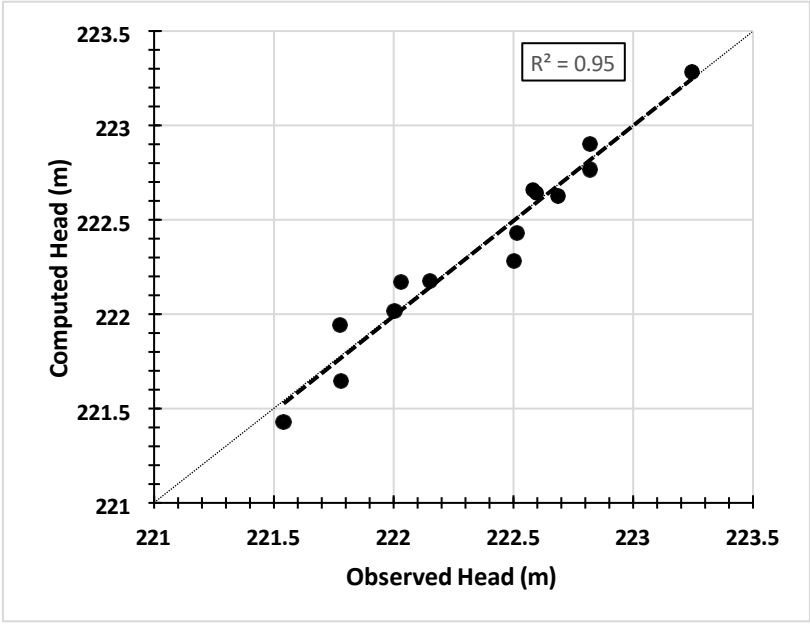

Figure 10: Plot showing observed versus computed hydraulic heads.

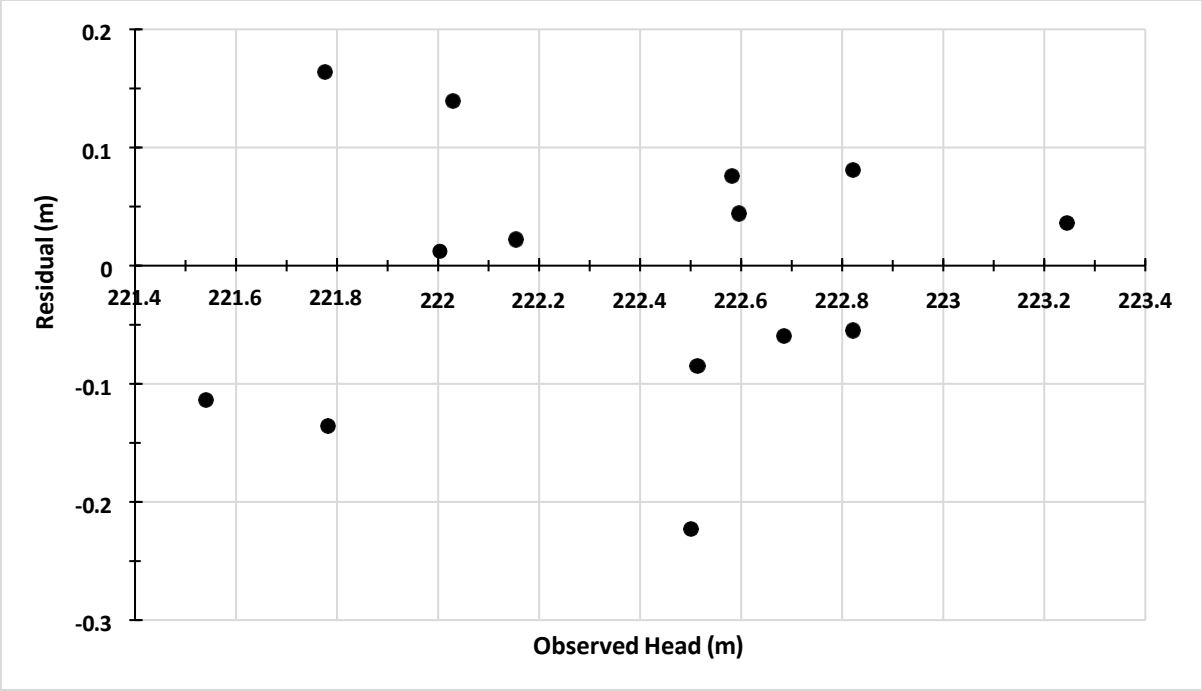

Figure 11: Plot showing residual versus observed hydraulic heads.

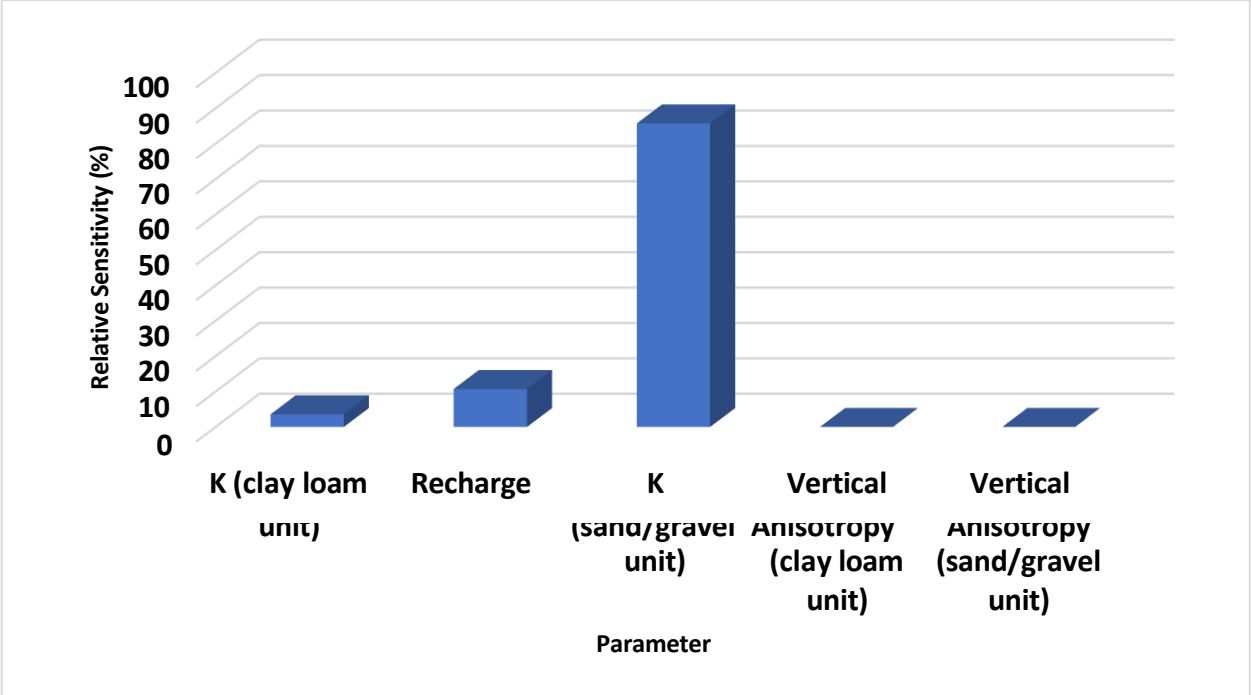

Figure 12: Relative sensitivity plot

Table 4: Post calibration parameters and values

Parameter	**Value**
Horizontal hydraulic conductivity - clay loam (m/day)	0.182
Horizontal hydraulic conductivity - sand/gravel (m/day)	Pilot Point (see Figure 12b)
Recharge (m/day)	0.000693
Vertical Anisotropy – clay loam	2.64
Vertical Anisotropy – sand/gravel	52.202

4.2 Model Uncertainty Quantification (Parameter Randomization)

The 47 equiprobable realizations of the subsurface yielded root mean square error heads ranging from 0.11 to 0.25 m. Recharge flux ranged from a minimum value of 0.000101 m/day to a maximum value of 0.000739 m/day with a mean value of 0.000292 m/day. Vertical anisotropy for the clay loam unit ranged from a minimum value of 1.071 to a maximum value of 96.170 with a mean of 26.185, while vertical anisotropy of the sand/gravel unit ranged from 1.098 to 87.54 with a mean of 15.484. The hydraulic conductivity of the clay loam unit ranged from a minimum value of 0.078 m/day to a maximum value of 0.513 m/day with a mean value of 0.189 m/day. Mean hydraulic conductivity distribution for the sand/gravel unit shows high values (highest: 100 m/day) at the northeast part of the study area and reduces moving in a southern direction (lowest: 1 m/day). The mean head and mean hydraulic conductivity for the sand/gravel interval is displayed in Figures

12(a) and 12(b), respectively. The mean hydraulic conductivity is same as that produced by calibration as the pilot points were interpolated using inverse distance weighted method, which is deterministic and as such does not provide an error range necessary for uncertainty quantification.

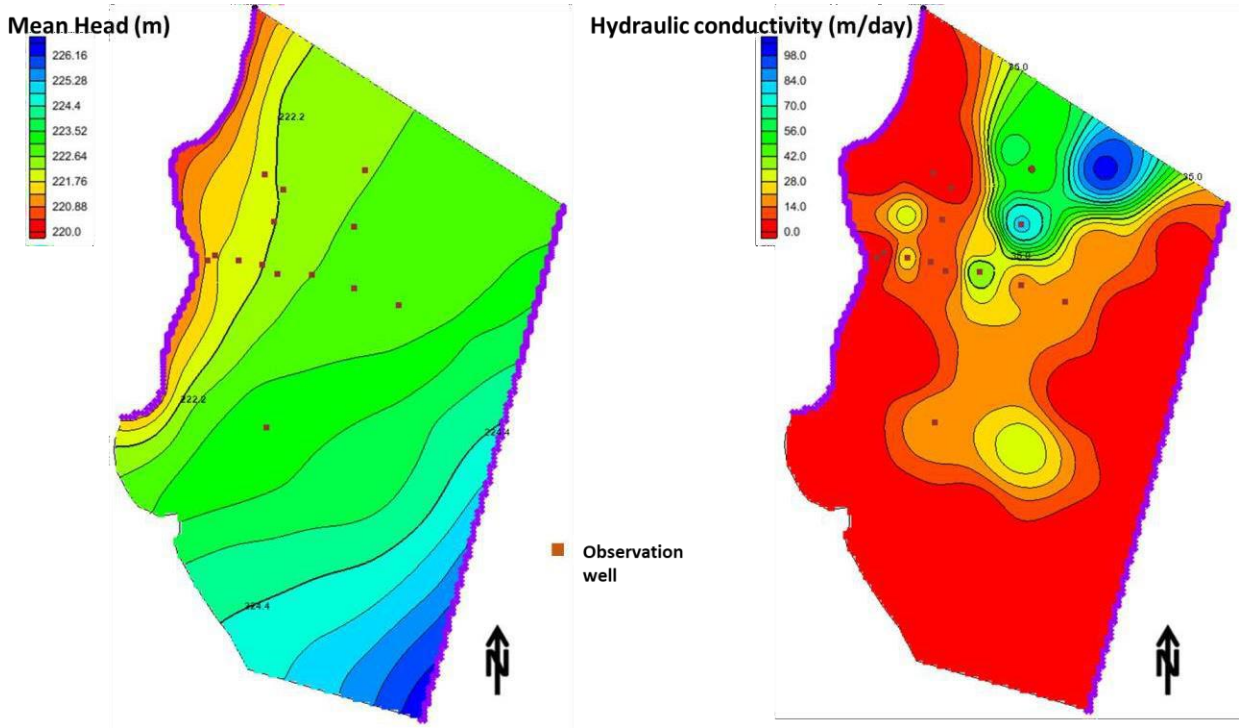

Figure 13: (a) Mean head (m) for sand/gravel unit (b) Mean hydraulic conductivity (m/day) for sand/gravel unit.

4.3 Scenario Analysis

At tile discharge of 40 m^3/day, particles at the injection wells originated from the eastern boundary of the model with contributing particle width of 64.3 m. The contributing particle width is defined as the distance measured side to side from where the particle originates (Figure 14).

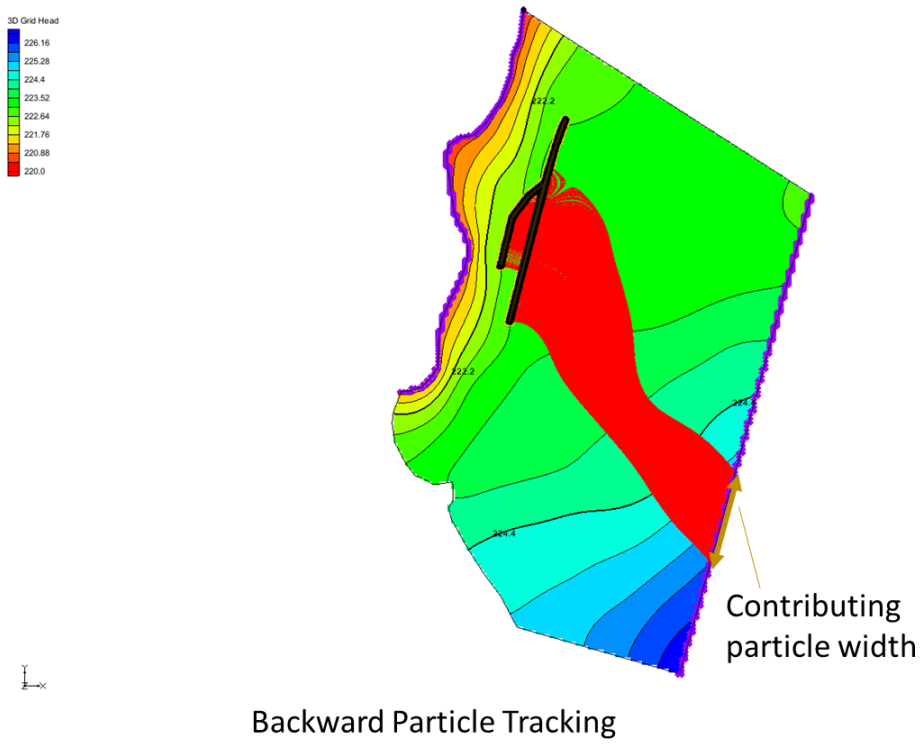

Figure 14: Picture showing defined contributing particle width.

This reduced to 50.9 m, and 2.61 m for 48 m^3/day and 100 m^3/day respectively, and at tile discharge of 200 m^3/day, the contributing area (cells) disappeared (Figure 15). A graph of groundwater contributing particle width versus tile discharge shows a negative nonlinear relationship with a coefficient of correlation of 0.98 (Figure 16).

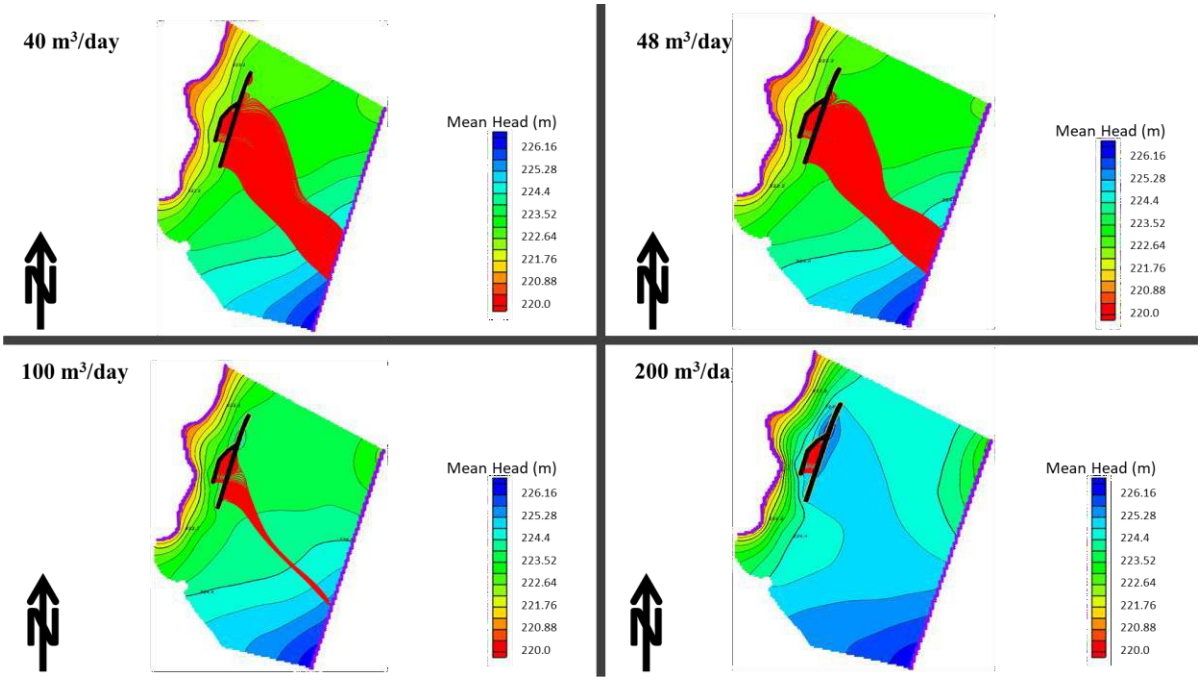

Figure 15: Picture showing backward particle flow path lines for 40 m^3/day, 48 m^3/day, 100 m^3/day and 200 m^3/day tile discharge, respectively.

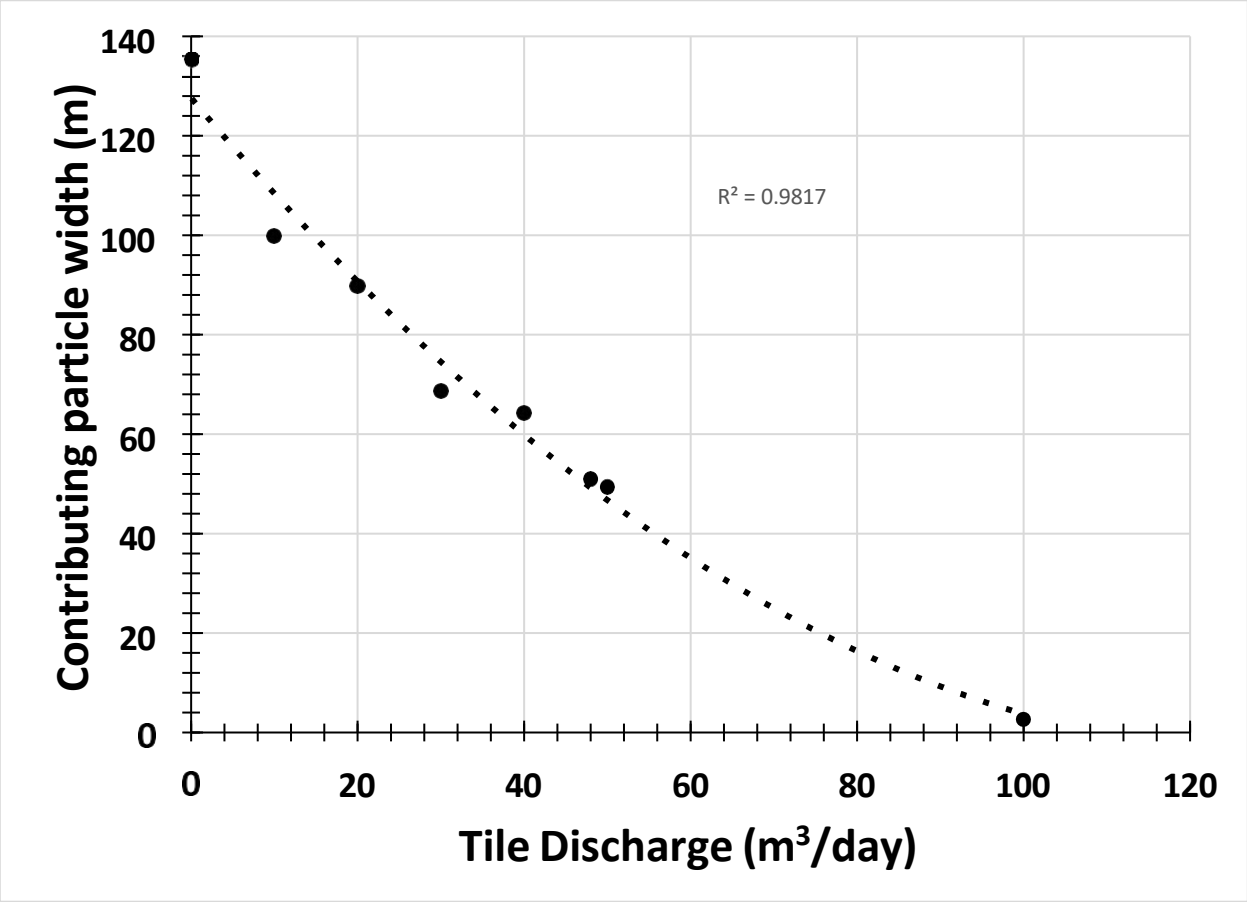

Figure 16: Plot showing groundwater contributing area per width versus tile discharge.

At tile discharge of 40 m^3/day, particles placed near diversion tiles saw a near field influence of 2.2 m because of particles moving around the groundwater mound developed from tile discharge. The near field influence is defined as the distance from the cell closest to the mid segment of the diversion tile to the point where the first backward run particle is deflected (Figure 17).

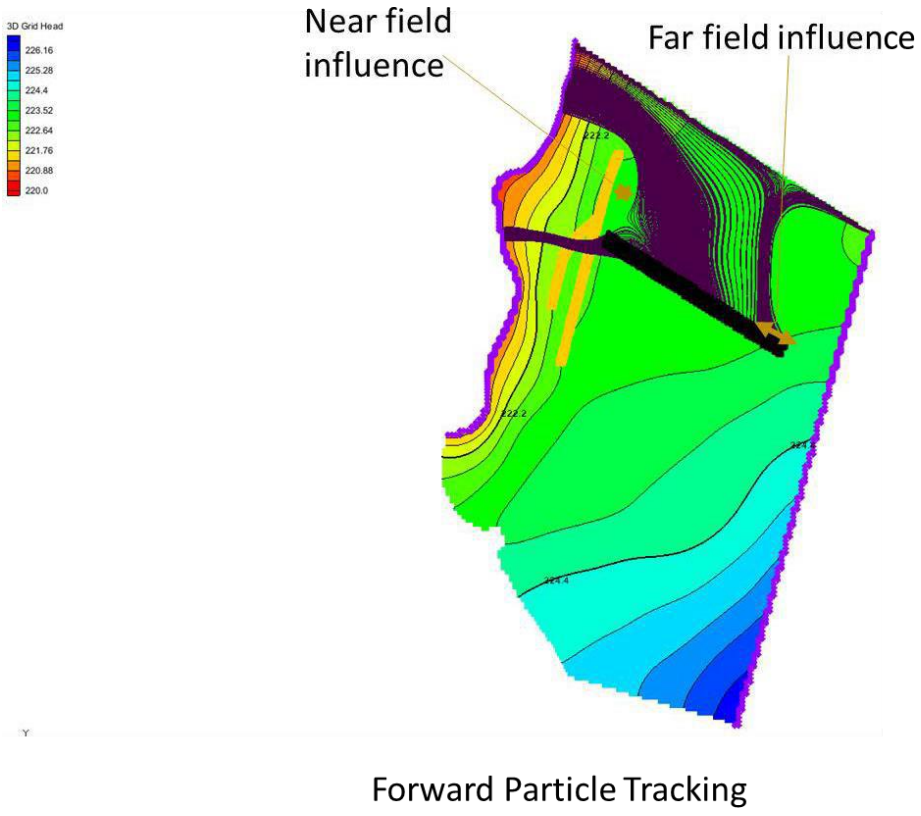

Figure 17: Picture showing defined near and far field influence

This field of influence increases to 10.8 m, 29.3 m, and 38.5 m at tile discharge of 48 m^3/day, 100 m^3/day and 200 m^3/day respectively (Figure 18). A graph of near field influence versus tile discharge shows a positive logarithmic relationship with coefficient of correlation of 0.96 (Figure 19).

At tile discharge of 40 m^3/day, particles placed near diversion tiles saw no far field influence because all particles were moving towards the stream. The far field influence is defined as the distance from the cell where the first forward run particle deflects to the east boundary to the last cell where the particle equally moves eastwards. The far field influence increases to 2.0 m, 74.6 m, and 106.2 m at tile discharge of 48 m^3/day, 100 m^3/day and 200 m^3/day respectively

(Figure 18). A graph of far field influence versus tile discharge shows a positive logarithmic relationship with coefficient of correlation of 0.97 (Figure 19).

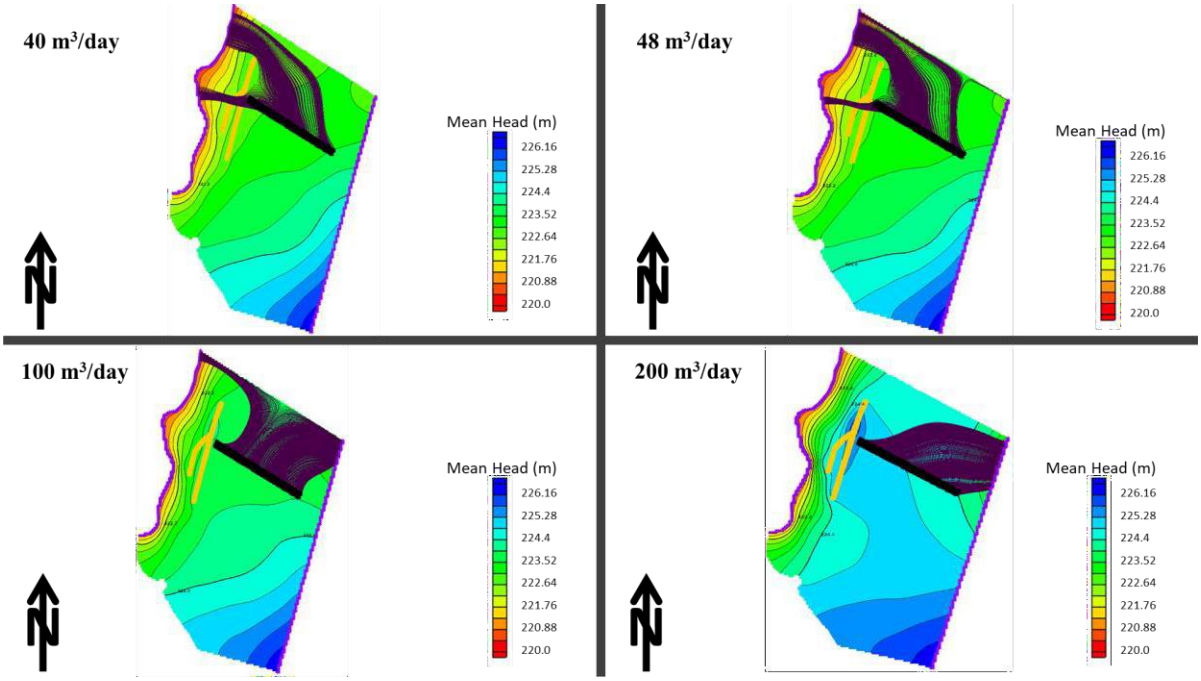

Figure 18: Figure showing near and far field particle path lines for 40 m^3/day, 48 m^3/day, 100 m^3/day, and 200 m^3/day tile discharges, respectively.

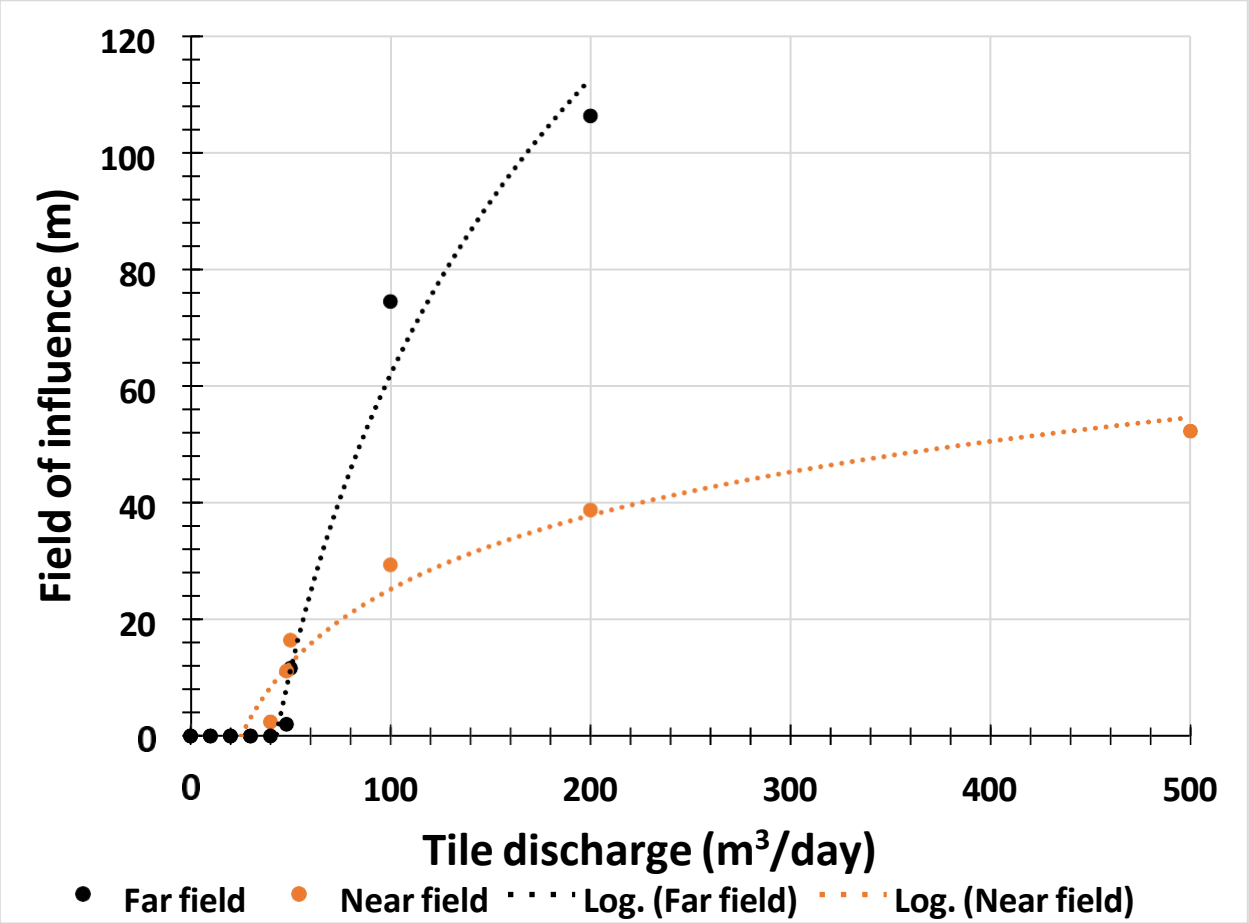

Figure 19: Plot showing the field of influence versus tile discharge.

CHAPTER V: DISCUSSION

5.1 Calibration

The use of pilot points and zonal based calibration approach against multiple sets of parameters allowed for the reproduction of hydraulic head as seen in the groundwater map in Sahad (2022), with root mean square of hydraulic head (0.11 m) lower than the observed head interval (0.2 m), except for well 19. This can be attributed to the error generated from assumption of uniform depth of the bottom of the clay loam unit. The pilot points enabled the production of heterogeneous hydraulic conductivity distribution in the sand/gravel unit that is typical of depositional environment of a glacial till. Calibrated model estimate of groundwater discharge into T3 stream is 61 m^3/day, which tallies with field measured estimates. Mean recharge of 0.000292 m/day is approximate to recharge value of 0.000261 m/day as reported in Van der Hoven et al (2008). However, the mean value of hydraulic conductivity of the clay loam unit (0.18 m/day) did not agree with field measured values (~1 m/day). This is attributed to the inherent variability in hydraulic conductivity of the clay loam interval, albeit at a smaller scale as compared to the sand/gravel interval. The mean hydraulic conductivity of the sand/gravel unit (between 1 m/day to 100 m/day) lies within range of that measured from slug tests (varying from 0.08 m/day to 210 m/day).

5.2 Scenarios

At 40 m^3/day, particles in the backward particle tracking model displayed a significant contribution to flow towards buffer zone as shown in particle flow field. This demonstrates the contribution of groundwater on the SBZ. The particle flow field continually decreases as tile

discharge increases and completely disappears at tile discharge greater than 100 m^3/day. This is because the groundwater mound is greater than contribution of groundwater flow and as such the effect of groundwater flow is no longer noticed at the SBZ. This has implications for nitrate reduction processes as this would mean that the effect of dilution reduces as tile water discharge increases.

At 40 m^3/day, all particles in the forward model migrated to the stream because groundwater mound isn't high enough to overcome influence of groundwater flow. The first particle deflects towards the farm field at 48 m^3/day, implying rate at which groundwater mound could potentially impact farm field. The quantity of particles increases significantly at 100 m^3/day and at the 200 m^3/day scenario, all particles migrate eastward. The results from forward particle tracking show that the field of influence of tile water increases at a nonlinear rate at near field (close to tile) and far field (close to the farm fields) as tile water discharge increases. This tallies to some extent with the expected result of a linear rate of increase of tile discharge versus field of influence. This has implications in terms of land management, as high rates of tile water discharge would entail larger area of farm fields prone to waterlogging. It also has implications in terms of nitrate transformation processes. This is because increased tile water discharge leads to development of groundwater mounds that transport nitrate laden tile water closer to the surface where it gets increased contact with the organic clay topsoil (Figure 17). This increased contact would aid nitrate reduction processes such as denitrification, thus improving the effectiveness of the SBZ.

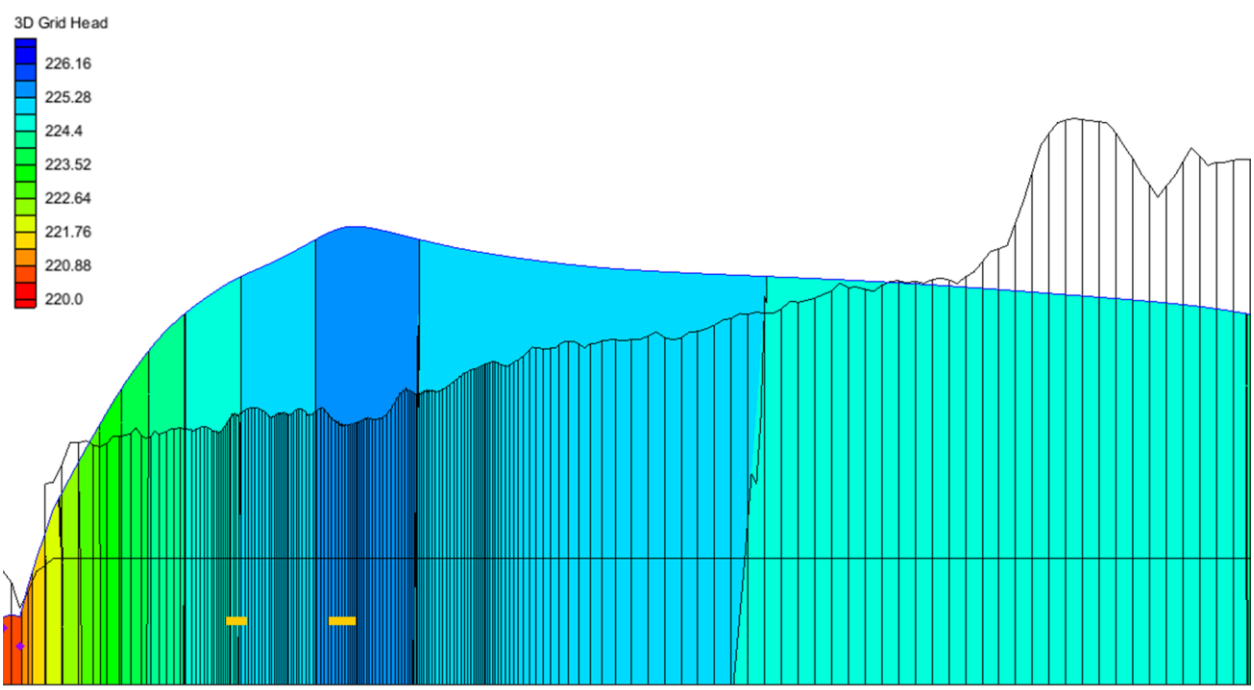

Figure 20: Cross-sectional view of groundwater model with tile discharge at 200 m^3/day (Exaggeration: X10)

5.3 Limitations

In the development of the conceptual model certain assumptions were made that increases uncertainty in the results of the numerical model. First, the bottom of the clay loam unit was estimated uniformly at 221.5 m while the bottom of the sand/gravel unit was estimated uniformly at 220.0 m. This assumption may not be held in the field and could alter the calibration and scenario results. There is also uncertainty as to the distribution of flow within the diversion tile. This would have an impact on the results of particle tracking that is significantly different from that assumed. The steady-state groundwater model built also assumes that tile flows consistently in each day which isn't the case. Uncertainty exists as to the specified head values at the eastern boundary, as it was estimated from the groundwater map that it doesn't extend all the way to the eastern boundary location. Lastly, the model was calibrated only with respect to the hydraulic head, as

there was no baseflow data at the time of data collection. This would affect the reliability of the calibration as the recommended practice for groundwater modeling is to use both head and flux observation data (Anderson et al, 2015).

CHAPTER VI: CONCLUSIONS

This study attempted to understand the interaction between groundwater flow and tile water in the SBZ. Finite difference groundwater modeling code (MODFLOW) was used to produce a three-dimensional steady-state groundwater flow model. After calibration using manual and autocalibration techniques, several scenarios with variable tile discharge were simulated, and the resulting change in groundwater flow direction using particle tracking code – MODPATH is analyzed. At variable tile discharge rates, the field of influence of the tile water was subsequently measured. The main findings of the study are as follows:

- the use of pilot points and zonal based calibration approach against multiple sets of parameters allowed for the reproduction of the observed hydraulic head,
- the influence of groundwater flow reduces in a nonlinear fashion as tile discharge increases, and
- the field of influence of tile water increases logarithmically as tile water discharge increases.

Further work is suggested in the following areas:

- development of a transient groundwater model calibrated using both streamflow and observed head as targets and preferably using MODFLOW-NWT that uses Newton-Raphson formulation for MODFLOW 2005 (Niswonger et al., 2011) to address the challenge of dry cells. The development of a transient model would also help address the challenge of inconsistency of tile flow in each day.

- use of head dependent boundary for the T3 stream in the transient model to better capture stream-groundwater interaction. This would require calibration of conductance of streambed and field measurement of stream stage.
- development of a reactive contaminant transport model to better understand the transport and fate of nitrate in the SBZ, by considering the effect of dispersion and other reactive processes.

REFERENCES

Anderson, T., Groffman, P., Kaushal, S., and Walter, M. 2014. Shallow Groundwater Denitrification in Riparian Zones of a Headwater Agricultural Landscape, Journal of Environment Quality, v. 43, p. 732-744, doi: https://doi.org/10.2134/jeq2013.07.0303

Anderson, M.P., Woessner, W.W., and Hunt, R.J., 2015. Applied Groundwater Modeling, 2nd Edition., 630. Amsterdam, Netherlands: Elsevier.

Bosompemaa, P., Peterson, E. W., Perry, W., and Seyoum, W. M. 2021. Recycling of nitrate and organic matter by plants in the vadose zone of a saturated riparian buffer: Water, Air, and Soil Pollution, v. 232, doi: https://doi.org/10.1007/s11270-021-05202-3.

Carpenter, S., Correll, D. L., Howarth, R. W., Sharpley, A.N., and Smith, V.H., 1998. Nonpoint pollution of surface waters with Phosphorus and Nitrogen, Ecological Applications, v. 8, p. 559-568, doi: https://doi.org/10.1890/1051-0761(1998)008[0559:NPOSWW]2.0.CO;2

Changnon SA, Angel JR, Kunkel KE, Lehmann CMB 2004. Climate atlas of Illinois. Illinois State Water Survey, Champaign, IL

Chen, D., and Macquarrie, K. 2004. Numerical simulation of organic carbon, nitrate, and nitrogen isotope behavior during denitrification in a riparian zone, Journal of Hydrology, v. 293, p. 235–254, doi: https://doi.org/10.1016/j.jhydrol.2004.02.002.

Chunjian L., Xiaojie L., Peng Y., Yonghui S., Hongjie G., Xiaoling L., Ruixia L., Huibin Y. 2021. Nitrogen retention effect of riparian zones in agricultural areas: A meta-analysis, Journal of Cleaner Production, v. 315, ISSN 0959-6526, https://doi.org/10.1016/j.jclepro.2021.128143.

Collman, R. D. 2004 Soil survey of McLean County, Illinois.

David, M.B., and Gentry, L.E., 2000. Anthropogenic inputs of nitrogen and phosphorus and riverine export for Illinois, USA: Journal of Environmental Quality, v. 29, p. 494–508, doi: https://doi.org/10.2134/jeq2000.00472425002900020018x

De Luca, D., and Lasagna, M. 2005. Aquifer role in reducing nitrate contamination by means of the dilution process, 6th International Conference "Sharing a common vision of our water resources" at: Menton, France, https://www.researchgate.net/publication/256444739_Aquifer_role_in_reducing_nitrate_contamination_by_means_of_the_dilution_process

Doherty, J. (2003), Ground Water Model Calibration Using Pilot Points and Regularization. Groundwater, 41: 170-177. https://doi.org/10.1111/j.1745-6584.2003.tb02580.x

Doherty, J. E. and Hunt, R. J. 2011. Approaches to Highly Parameterized Inversion – A Guide to Using PEST for Groundwater-Model Calibration: U.S. Geological Survey Scientific Investigations Report 2010–5169, p. 59. https://doi.org/10.3133/sir20105169

Doherty, J. E. 2020a. Model-Independent Parameter Estimation User Manual Part II: PEST Utility Support Software. Watermark, Brisbane, Australia, p. 268

Doherty, J. E. 2020b. PEST: Model-Independent Parameter Estimation and Uncertainty Analysis—User Manual Part I. Watermark, Brisbane, Australia, p. 394.

Eby, G.N. (2004). Principles of Environmental Geochemistry. Brooks/Cole, 514p.

Galloway, J., Townsend, A., Erisman, JW., Bekunda, M., Cai, Z., Freney, J., Martinelli, L., Seitzinger, S., and Sutton, M. 2008. Transformation of the Nitrogen Cycle: Recent Trends, Questions, and Potential Solutions, Science, v.320, p. 889-892, doi: https://doi.org/10.1126/science.1136674.

Groh, T.A., Davis, M.P., Isenhart, T.M., Jaynes, D.B. and Parkin, T.B. 2019. In Situ Denitrification in Saturated Riparian Buffers, Journal of Environmental Quality., v.48, p.376-384, doi: https://doi.org/10.2134/jeq2018.03.0125

Hill, A.R. 1996. Nitrate Removal in Stream Riparian Zones, Journal of Environmental Quality, v. 25, p. 743-755, doi: https://doi.org/10.2134/jeq1996.00472425002500040014x

Hunt, R.J., Doherty, J. and Tonkin, M.J. 2007. Are Models Too Simple? Arguments for Increased Parameterization. Groundwater, 45: 254-262. https://doi.org/10.1111/j.1745-6584.2007.00316.x

Jaynes, D.B., and Isenhart, T. M. 2014. Reconnecting Tile Drainage to Riparian Buffer Hydrology for Enhanced Nitrate Removal, Journal of Environmental Quality, v. 43, no. 2, p. 631-638, doi: https://doi.org/10.2134/jeq2013.08.0331

Jaynes, D.B. and Isenhart, T. 2019a. Performance of Saturated Riparian Buffers in Iowa, USA,

Journal of Environment Quality, v. 48, p. 289-296, doi: https://doi.org/10.2134/jeq2018.03.0115

Jaynes, D.B. and Isenhart, T. 2019b. Increasing infiltration into saturated riparian buffers by adding additional distribution pipes, Journal of Soil and Water Conservation, v. 74 (6), p. 545-553, doi: https://doi.org/10.2489/jswc.74.6.545

Lasagna, M., De Luca, D., Debernardi, L., and Clemente, P. 2013. Effect of the dilution process on the attenuation of contaminants in aquifers. Environmental earth sciences, v. 70, p. 2336-2339, doi: https://doi.org/10.1007/s12665-013-2336-9

Lasagna, M., De Luca, D.A. and Franchino, E. 2016. The role of physical and biological processes in aquifers and their importance on groundwater vulnerability to nitrate pollution. Environmental Earth Sciences, v. 75, doi: https://doi.org/10.1007/s12665-016-5768-1

Ludwikowski, J. J., and Peterson, E. W., 2018, Transport and fate of chloride from road salt within a mixed urban and agricultural watershed in Illinois (USA): assessing the influence of chloride application rates: Hydrogeology Journal, v. 26, no. 4, p. 1123-1135, doi:10.1007/s10040-018-1732-3.

Manahan, S. E. 2010. *Environmental Chemistry*, *9th Edn*. Boca Raton, FL: CRC Press, 166–72

Mastrocicco, M., Boz, B., Colombani, N., Carrer, G.M., Bonato, M. and Gumiero, B. 2014. Modelling groundwater residence time in a sub-irrigated buffer zone. Ecohydrol., 7: 1054-1063. https://doi.org/10.1002/eco.1437

Mayer, P.M., Reynolds, S.K., McCutchen, M.D. and Cranfield, T.J., 2006. Riparian buffer width, vegetative cover and nitrogen removal effectiveness: A review of current science and regulations. EPA/600/R-05/118. Cincinnati, OH, U.S. Environmental Protection Agency

McEachran, A.R., 2020. Improving the design of saturated riparian buffers for removing nitrate from subsurface drainage. Graduate Theses and Dissertations. 18185. https://lib.dr.iastate.edu/etd/18185

McEachran, A. R., Dickey, L. C., Rehmann, C. R., Groh, T. A., Isenhart, T. M., Perez, M. A., and Rutherford, C. J. 2020. Improving the effectiveness of saturated riparian buffers for removing nitrate from subsurface drainage, Journal of Environmental Quality, v. 49, no. 6, p. 1624-1632, doi: https://doi.org/10.1002/jeq2.20160

McPhillips, L.E., Groffman, P.M., Goodale, C.L. and Walter, M.T. 2015. Hydrologic and Biogeochemical Drivers of Riparian Denitrification in an Agricultural Watershed, Water, Air and Soil Pollution, v. 226**,** no. 169, doi: https://doi.org/10.1007/s11270-015-2434-2

Miller, J., Peterson, E.W. and Budikova, D. 2018. Diurnal and seasonal variation in nitrate-nitrogen concentrations of groundwater in a saturated buffer zone, Journal of Hydrogeology, v. 27**,** p. 1373–1387, doi: https://doi.org/10.1007/s10040-018-1907-y

Molénat J. and Gascuel-Odoux C. 2002 Modelling flow and nitrate transport in groundwater for the prediction of water travel times and of consequences of land use evolution on water quality, Hydrological Process v. 16(2), p. 479–492, doi: https://doi.org/10.1002/hyp.328

Mondal, NC., Singh, V., and Rangaranjan, R., (2009). Aquifer characteristics and its modeling around an industrial complex, Tuticorin, Tamil Nadu, India: A case study. Journal of Earth System Science, v. 118, p. 231-244, doi: http://dx.doi.org/10.1007/s12040-009-0017-6

Moran, J. E., Tompson, A. B., Carle, S. F., Hudson, G. B., Esser, B. K., Kane, S. R., McNab, W. W., Beller, H. R., Lawrence Livermore National Laboratory, and United States. Department of Energy. 2004. Simulation of nitrate biogeochemistry and reactive transport in a california groundwater basin. United States. Dept. of Energy. Retrieved September 7, 2022, from http://www.osti.gov/servlets/purl/15013885-jg7OA1/native/.

National Crop Insurance Services. 2017. Agriculture Drives Illinois' Economy https://cropinsuranceinamerica.org/illinois/ (accessed 18th October 2021).

Niswonger, R. G., Panday, S. and Ibaraki, M. 2011. MODFLOW-NWT, A Newton Formulation for MODFLOW-2005: U.S. Geological Survey Techniques and Methods 6–A37, p. 44

Peoples, M. B., Herridge, D. F., and Ladha, J. K. 1995. Biological nitrogen fixation: an efficient source of nitrogen for sustainable agricultural production? Plant and Soil, v. 174, p. 3–28. doi: https://doi.org/10.1007/BF00032239

Pollock DW. 1994. User's guide for MODPATH: a particle tracking post-processing package for MODFLOW, the USGS finite-difference groundwater flow model. US Geological Survey Report.

Reilly, T.E., and Harbaugh, A.W., 2004. Guidelines for evaluating ground-water flow models: U.S. Geological Survey Scientific Investigations Report 2004-5038, 30 p. https://doi.org/10.3133/sir20045038

Rivett, M., Buss, S., Morgan, P., Smith, J., and Bemment, C. 2008. Nitrate Attenuation in Groundwater: A Review of Biogeochemical Controlling Processes, Water research, v. 42, p. 4215-32, Doi: https://doi.org/10.1016/j.watres.2008.07.020

Rosenstock, T., Liptzin, D., Dzurella, K., Fryjoff-Hung, A., Hollander, A., Jensen, V., King, A., Kourakos, G., Mcnally, A., Pettygrove, S., Quinn, J., Viers, J., Tomich, T., and Harter, T. 2014. Agriculture's Contribution to Nitrate Contamination of Californian Groundwater (1945–2005), Journal of Environmental Quality, v. 43, p. 895-907, doi: https://doi.org/10.2134/jeq2013.10.0411

Sahad, Alhassan (2022) "Using a tracer test to assess the transport and fate of nitrate within a saturated buffer zone, University *Research Symposium*. 374. https://ir.library.illinoisstate.edu/rsp_urs/374

Streeter, M.T., and Schilling, K.E. 2021. Quantifying the effectiveness of a saturated buffer to reduce tile NO_3-N concentrations in eastern Iowa, Environmental Monitoring and Assessment, v. 193, doi: https://doi.org/10.1007/s10661-021-09297-3

Tesoriero, A., Liebscher, H., and Cox, S., 2000. Mechanism and Rate of Denitrification in an Agricultural Watershed: Electron and Mass Balance Along Groundwater Flow Paths, Water Resources Research, v. 36, p. 1545-1559. Doi: https://doi.org/10.1029/2000WR900035

Ucisik, A.S., and Henze, M., 2004. Biological denitrification of fertilizer wastewater at high chloride concentration. Water SA, v. 30, no. (2), p. 191–195, doi: https://doi.org/10.4314/wsa.v30i2.5063

USDA-NASS. 2017. Publications. https://www.nass.usda.gov/Publications/AgCensus/2017/Online_Resources/County_Profiles/Illinois/ (accessed 18th October 2021).

Van der Hoven, S. J., Fromm, N. J., and Peterson, E. W., 2008. Quantifying nitrogen cycling beneath a meander of a low gradient, N-impacted, agricultural stream using tracers and

numerical modelling: Hydrological Processes, v. 22, no. 8, p. 1206-1215, doi:10.1002/hyp.6691.

Vidon, P., and Hill, A.R. 2005. Denitrification and patterns of electron donors and acceptors in eight riparian zones with contrasting hydrogeology, Biogeochemistry, v. 71, p. 259–283, doi: https://doi.org/10.1007/s10533-005-0684-6

Weedman, N.R., Malone, D.H., and Shields, W.E., 2014. Surficial Geologic Map of the Normal West 7.5 Minute Quadrangle, McLean County, Illinois: Illinois State Geological Survey, Student Map series, scale 1:24,000, https://www.isgs.illinois.edu/sites/isgs/files/maps/isgs-quads/normal_west_sg_ISU.pdf

Zarnetske, J., Haggerty, R., Wondzell, S., and Baker, M. 2011. Dynamics of nitrate production and removal as a function of residence time in the hyporheic zone, Journal of Geophysical Research (Biogeosciences), v. 116, G01025, doi: https://doi.org/10.1029/2010JG001356

APPENDIX

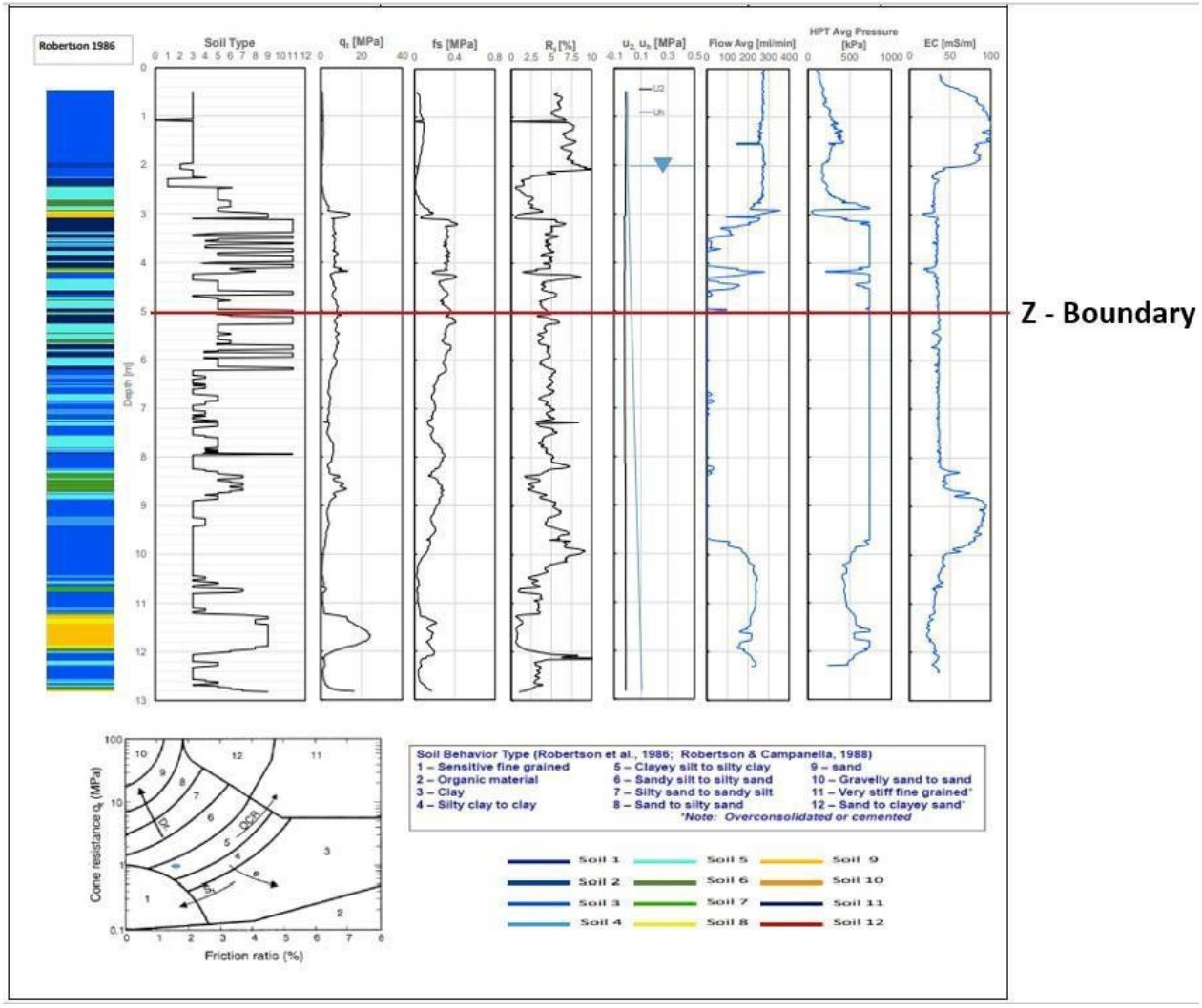

Figure 1: Cone Penetrometry and Hydraulic Profile data with red line depicting Z – Boundary (Courtesy Illinois State Geological Survey)